A Thesis

entitled

Evaluation of Remaining Fatigue Life of a Non-Cantilever Highway Truss With Tubular Joints

by

Abdullah Haroon

Submitted to the Graduate Faculty as partial fulfillment of the requirements for the

Master of Science Degree in

Civil Engineering

____
Dr. Serhan Guner, Committee Chair

____
Dr. Douglas K. Nims, Committee Member

____
Dr. Luis A. Mata, Committee Member

____
Dr. Cyndee Gruden, Dean
College of Graduate Studies

The University of Toledo

May 2019

An Abstract of

Evaluation of Remaining Fatigue Life of a Non-Cantilever Highway Truss With Tubular Joints

by

Abdullah Haroon

Submitted to the Graduate Faculty as partial fulfillment of the requirements for the Master of Science Degree in
Civil Engineering

The University of Toledo
May 2019

Non-cantilevered support structures have been widely used in the transportation department for supporting overhead traffic signs and signals. Several of them exhibit fracture failure at the welded connections, with the most likely cause being fatigue failure due to wind-induced vibrations. The failure usually occurs at “T”, “Y”, “K” tube to tube welded connections. The crack initiates at the welded junction of chord and diagonal and propagates circumferentially. A similar crack was observed at a truss on Alum Creek Drive at the interchange of I-270 in the state of Ohio. An investigation, funded by ODOT, was conducted at the University of Toledo into the cause of failure.

Finite element modeling of the structure was conducted using SAP2000. External loadings from natural wind gusts were considered. It was presumed that the effects of other loadings such as vortex shedding, galloping, and truck gusts are negligible for this structure. Both static and transient dynamic analyses were performed. Weather data of daily variation in wind speed and direction were obtained from NCDC and a probabilistic wind distribution was performed. Using Kaimal spectrum load time histories of natural wind was generated, and a transient dynamic analysis was performed. Stress histories of

critical members were extracted, and Palmgren-Miner rule was applied to evaluate the fatigue life of the critical members. The analysis results indicated that if the weld is assumed to be of sound quality, the fatigue life of the critical members under the effect of natural wind gust greater than the service life of the truss.

Simulated damage scenarios were introduced by reducing the load carrying capacity of the members at failed joints and fatigue life was compared in undamaged and damaged states. Damage was introduced by reducing the mechanical strength of failed members and deterioration due to poor weld quality was not considered Compared to the undamaged state, the fatigue life in all the three damage scenarios was found to reduce by only 10%. This suggests that assuming the welds are done as per code requirements, the truss is redundant enough to sustain some damage without affecting the overall fatigue life of the structure.

Even though the findings of this report predict the fatigue life to be greater than the service life of the truss, it should be noted that this result is only valid with the presumption that welded connections between members of the truss are sound and no defect in weld quality is considered in the present analysis. A quantitative assessment of the effects of weld defects on the fatigue life of the structure could give a better understanding of the failure mode, but such a venture was beyond the scope of this study.

Dedicated to my family and friends without whom none of my success would ever be possible.

Acknowledgements

First and foremost, the praise is due to almighty ALLAH for His unconditional grace and benevolence that allowed me to excel in all my academic pursuits.

With immense pleasure and gratitude, I acknowledge my amiable and ever supporting research advisors Dr. Serhan Guner and Dr. Douglas Nims for their guidance and insight during the entire duration of this project. I would like to express sincere thanks to all the committee members for their time and valuable comments on the thesis. Lastly, I would like to appreciate the efforts and support of family, friends and fellow graduate students who were directly or indirectly involved in successful completion of this thesis.

Table of Contents

List of Tables

List of Figures

Chapter 1

Introduction

1.1 Motivation

Sudden failure of an in-service non-cantilever highway truss on Alum Creek Drive at the interchange of Interstate 270 lead Ohio DOT to initiate an investigation to determine the cause of failure and whether it is a systematic problem that needs to be addressed. A research team from the University of Toledo, Ohio, conducted a study including both qualitative electron microscopy and analytical fatigue life evaluation due to natural wind gust. Only the analytical portion of the investigation is discussed in this report.

Non-cantilevered highway structures have been widely used by state DOTS over many decades to support traffic signs, signals and luminaries. The configuration of these non-cantilevered support structures has developed gradually but many of them, currently in service, structures are box type four chord trusses with fully welded tubular connections. Such structures are often subjected to cyclic loading due to natural wind gusts or gusts from passing traffic underneath. A well-recognized problem reported by several state DOTs is the performance of the welded tubular joints at the chord-diagonal intersections (Schumacher et al. 2009). Due to different cross sections of the intersecting members, the stiffness of the joints is typically variable (Schumacher et al. 2009), which results in non-uniform stress distributions at these joints when subjected to cyclic loading. Several DOTs have reported cracks at “T”, “Y”, and “K” tube-to-tube welded connection of such trusses, well before the end of their design life (Ginal 2003)(Foutch et al. 2006). In most of these cases, the failure was attributed to fatigue due to excessive vibrations caused by wind and/or truck gusts.

The assessment procedures contained in AASHTO specifications (AASHTO 2015) are not fully applicable to this particular problem. AASHTO specifications propose the use of nominal stress-based S-N curve method to assess the remaining fatigue life of highway trusses. This procedure requires the pre-categorization of weld details and establishing the fatigue resistance (S-N curve) of these pre-defined weld details through laboratory testing (Maddox 2003). The AASHTO specifications classify the tubular joints of non-cantilevered trusses in the ‘ET’ category with one of the lowest fatigue resistances, however, the specifications do not provide S-N curve for ‘ET’ weld details but merely provide the constant amplitude fatigue limit (CAFL) for the weld detail, which presumably corresponds to ‘adequate’ fatigue life. Huckelbridge et al. (Huckelbridge 2009) analytically estimated the S-N curve for ‘ET’ category based on curve fitting method and is used for this investigation.

Also, the fatigue resistance (S-N curve) of these tubular connections, unlike other details, has not been established based on laboratory testing but corresponds to classification specified by the AWS Structural Welding Code (AASHTO 2015). AWS classifications (American Welding Society 2015) are based on research in offshore industry, performed on connections of thicker and larger diameter tubes. However, since the stresses in tubular connections depend strongly on the geometric parameters of the tubes, such extrapolation from AWS specifications may not be consistent for the current slender connections in service. Independent researchers (MASHIRI 2007) (Schumacher 2009) have established the 'size effect' corrections for tubular joints but their considerations in design codes are limited.

ODOT has jurisdiction over several non-cantilevered support structures that have shown in-service problems. Majority of these problems are concerning the welded tubular connections at the chord-diagonal junction. Generally, circumferential cracks are found within the leg or toe of the fillet weld at the chord-diagonal joint. Depending upon the time it has to grow, the crack can propagate into the chord and can cause the collapse of total or a part of the structure. Such an event could have catastrophic consequences on any busy highway. While locating these cracks through routine inspections and preventing any unforeseen failure is the first step in addressing the problem, determining the actual cause(s) of the failure is important to better understand the problem and develop possible fixes.

The scope of the investigations involved three separate tasks: (1) An analytical evaluation of fatigue life due to wind (presented in this thesis); (2) Effect of diurnal temperature variations and HAZ (KC 2019); (3) Material characterization of regions with and without failure, using electron microscopy (Nims 2019).

1.2 Objective of study

The decommissioned non-cantilevers truss on Alum Creek Drive at the interchange of Interstate 270 was used as the representative structure for this study. The truss experienced a fracture failure at the two ends of its chord. An investigation into the cause of failure was undertaken with the following objectives:

a) Develop an analytical model of the truss to compute the response of truss to natural wind gust.
b) Based on AASHTO (AASHTO 2015), calculate design load capacity and fatigue resistance of the truss and check if the design is adequate.
c) Identify the members prone to fatigue failure and evaluate their fatigue life.
d) Evaluate the fatigue life of the truss under simulated damage scenarios and compare it with the fatigue life in the undamaged state.

1.3 Thesis organization

Chapter 1- Introduction presents a brief overview of this study. Motivation to undertake this study is described and the objectives of the research are stated.

Chapter 2- Literature review sheds some light on the development of regulations for the support structures. A brief background of analytical wind engineering and fatigue analysis procedures is discussed.

Chapter 3- Structural analysis describes the representative truss and observations made during the field inspection of the truss. Finite element model developed for the truss and static analysis of performed is also discussed in detail.

Chapter 4- Fatigue analysis details the procedure employed to calculate the fatigue life of the structure. Included in this chapter are the results of the wind speed distribution, wind load time history, stress time history of critical members and fatigue life of these members. Simulated damage scenarios are explained, and fatigue life of damages states is calculated and compared with the undamaged state.

Chapter 5- Conclusion: This chapter presents a summary of results from the study and suggestions are made for future work.

Chapter 2

Background

This chapter aims at summarizing the development of regulations for highway sign support structures. The National Cooperative Highway Research Program (NCHRP) has undertaken several projects to help and improve the American Association of State Highway and Transportation Officials (AASHTO) standard and guidelines for the highway sign support structures. Pertinent research from these reports along with their effects on AASHTO guidelines is discussed in section 2.1. Section 2.3 outline the process of analytical wind engineering and section 2.5 describes fatigue life evaluation method.

2.1 Development of regulations

After several incidents of fatigue failure in highway sign structures were reported, engineers realized that 1994 AASHTO Standard Specifications for Structural Supports for Highway Signs, Luminaries and Traffic Signals (henceforth referred to as *Support specifications*) needs revision to guard against fatigue. The response of these structures under wind load and fatigue resistance of various connections details need to be well understood. NCHPR Project 10-38 "Fatigue –Resistance Design of Cantilever Signals, Signs, and Light Supports," was started and extensive experimental and analytical work was performed to develop guidelines to prevent excessive vibrations and fatigue of cantilevered sign, signals and light support structures. Findings of the research were issued in the form of NCHPR report 412 (Kaczinski et al. 1998). The project was aimed at identifying wind-loading phenomena critical to fatigue failure, identifying fatigue sensitive connection details, develop fatigue limit-state wind loads and identifying fatigue strength of anchor bolts.

Four wind loads, i.e. galloping, vortex shedding, natural wind gust, and truck induced wind gusts were identified as potential sources that can cause large amplitude vibrations and can cause fatigue failure. Wind tunnel tests were performed to quantify the dynamic response of cantilevered signs and signal structures under galloping and vortex shedding phenomena. Magnitudes of equivalent static fatigue limit-state loads for galloping, vortex shedding, and natural wind gust were estimated by performing static and dynamic finite element analyses. A simple static load model for truck-induced wind gust was validated using analytical calculations.

Fatigue sensitive connection details were identified with the help of standard drawings from the state department of transportation and manufacturer literature. These details, based on their cracking mode and stress concentration, were categorized, according to AASHTO (AASHTO 2012) and AWS (American Welding Society 2015) fatigue design curves, from A to E' where the fatigue threshold decreases as we move from A to E'. Several details for cantilevered support structures were found to have very low fatigue strengths and were categorized into E or E'.

The fatigue chapter of the AASHTO 1994 supports specifications was updated based on the recommendations of NCHRP report 412 and contains provisions for the fatigue design of cantilevered steel structural supports. These supports should be designed for fatigue due to loads from galloping, natural wind gusts, and truck induced wind gusts.

Despite the extensive research performed in NCHRP report 412, several issues needed further considerations or refinements. Until this point, all the research efforts were limited to cantilevered overhead support structures. Another NCHRP project was undertaken to enhance the support specifications and provide a strategic plan for future development of the specifications. As a result of this project, NCHRP report 494 (Fouad et al. 2003) was published in 2003. One of the core objectives of the work of Fouad et al. was to address fatigue and vibrations in non-cantilevered support structures. As a part of the project, a survey was sent by the research team to various state DOTs enquiring about the problems encountered with highway signs. Out of the 48 replies received, eight reported issues related to non-cantilevered support structures. An in-depth analytical investigation using the finite element method was conducted to establish equivalent static loads for non-cantilevered supports. Related issues such as connection details to minimize fatigue effects, the effect of gusset plates, and methods to mitigate vibrations were also addressed in the report. Following recommendations for fatigue loads on non-cantilevered supports came out of the report:

1. Galloping: A 21-psf shear pressure applied vertically to the projected area of the sign mounted over monotube as viewed in the elevation. Galloping needs to be considered only for horizontal monotubes. Non-cantilevered support structures are excluded.

2. Vortex shedding: Use the same model for non-cantilever supports as present in NCHRP report 412 for cantilever supports. This requirement can be disregarded if signs or sign blanks are used during construction.
3. Natural wind load: A pressure range of 5.2-psf multiplied by the drag coefficient applied horizontally to the exposed area.
4. Truck induced loads: Horizontal pressure of 7.5-psf applied to the area of the sign and the area of the support structures, and the vertical pressure of 10.2-psf applied to the area of the support structure and the projected area of the sign. These loads should be applied along 24 feet or entire span, whichever is smaller.

2.2 Previous studies

Efforts have been made to address the overall fatigue performance of non-cantilevered signs such as NCHRP Report-494 (Fouad 2003); however, special attention for tubular details is required. Several state-funded programs have attempted to address this issue but resulted in varying conclusions such as weld defects, truck gust vibration, infinite life, etc. Such studies varied by the type of wind loading, the dimensions, and type of the truss, analytical modeling of wind, and the method of transient dynamic analysis.

Ginal (Ginal 2003) evaluated the fatigue performance of three overhead box-type trusses. The effect of wind load and truck gust were determined separately. The fatigue life of critical members was found to vary in the range of four to twenty-seven years. Li (Li et al. 2006) utilized ANSYS to model the critical connections in a box truss. Unlike Ginal (Ginal 2003), he found the fatigue life of all the connections in the box truss to be infinite. Huckelbridge (Huckelbridge and Metzger 2009) analyzed a bridge mounted overhead sign support along Interstate 75 in Dayton (Ohio) after a complete failure of two truss members was noted during a field inspection. A combination of in-situ field monitoring of the traffic induced bridge vibrations along with analytical modeling of the truss was carried out. The investigation concluded that the failure was due to extreme high-cycle fatigue caused by vibrations due to traffic.

2.3 Wind Engineering

2.3.1 Dynamic wind loads on sign structures

Wind is a non-periodic dynamic action that fluctuates over time. Its effect on the structure is dependent upon its direction, speed and shape and height of the structure. These variables combine to induce several different actions that can cause large amplitude vibrations in the structure and cause damage.

Experimental and analytical research performed in NCHPR report 412 identified four wind loading phenomenon as possible sources that can cause large amplitude vibrations and cause fatigue failure, i.e. vortex shedding, galloping, natural wind gusts and truck induced wind gusts. These phenomena were established only for cantilever structures and non-cantilevered structures were out of the scope of NCHPR-412.

Galloping is an aerodynamic phenomenon that arises due to varying angle of wind attack on the structure. It is characterized by large amplitude oscillations perpendicular to wind flow. Galloping is found to be critical in flexible structures with a low natural frequency such as cantilevered sign supports.

Vortex shedding, like galloping causes vibrations normal to wind direction. When a steady uniform wind flow passes a bluff body, vortices are created at the back of the body and detach periodically on either side of the body creating alternate low-pressure zones. The structure tends to move towards the low-pressure zone and oscillates normal to the direction of the wind.

Truck induced wind gusts are produced when heavy vehicles pass under the overhead sign at high speeds. As the vehicle passes the structure, a wind gust is induced in both vertical and horizontal directions that strike the structure and causes oscillations. Horizontal gust induced by truck, as compared to natural wind, is so small to be negligible. Vertical pressure greatly depends on the height of the structure and area parallel to the road.

Natural wind gust is the most significant contributor to fatigue damage to overhead signs. The random nature of natural wind causes non-periodic oscillations in the structure causing fatigue damage. The magnitude of these natural wind forces depends on several factors such as speed of the wind, its direction, height and shape of the structure, etc.

Both galloping, and vortex shedding are not significant for non-cantilevered structures and hence are not considered in this study. Truck induced wind gusts are noticeable for non-cantilevered structures, but their occurrence is much less compared to natural wind gusts (Li 2006). Hence, in this research, it is assumed that natural wind gust is the primary contributor to fatigue damage in the structure.

2.3.2 Natural wind

To accurately measure the dynamic effect of wind on any structure, a function of wind speed variation with time is required. Due to its gustiness characteristic, the wind can be described as a random vector field whose speed and direction at any point in space changes continuously. At any point in the field, the instantaneous velocity of wind can be considered as a resultant of two components: a mean component $\bar{v}$, and a fluctuating component $v(t)$ that represents the turbulence.

The mean component is the steady flow velocity and is subjected to slow changes. Near the surface of the earth, the mean component varies with height above ground. Two empirical relations commonly used to describe the variation of the mean component with elevation are the Logarithmic law and the Power law. These relations are expressed mathematically in the following equations.

Power Law:

$$V(z) = V_1 \left(\frac{z}{z_1}\right)^{\alpha} \tag{2.1}$$

Logarithmic Law:

$$V(z) = \frac{1}{k} V_* ln\left(\frac{z}{z_o}\right) \tag{2.2}$$

In the above equations $V(z)$ is the speed of wind at height z above the ground, V_1 is the reference speed at reference height z_1, α is the power law exponent based on terrain (generally smoother terrains have smaller value of α than rough terrains), V_* is the shear velocity, k is von Karman constant, z_o is ground roughness constant for Logarithmic law.

Logarithmic law is more difficult to use than Power law and sometimes may produce negative velocity when the height of the structure is less than the constant z_o, therefore Power law is preferred for most engineering applications. However, both the

Power law and the Logarithmic law produce very similar profiles at low heights. Figure 2-1 shows the comparison of the wind profiles generated by the two relations.

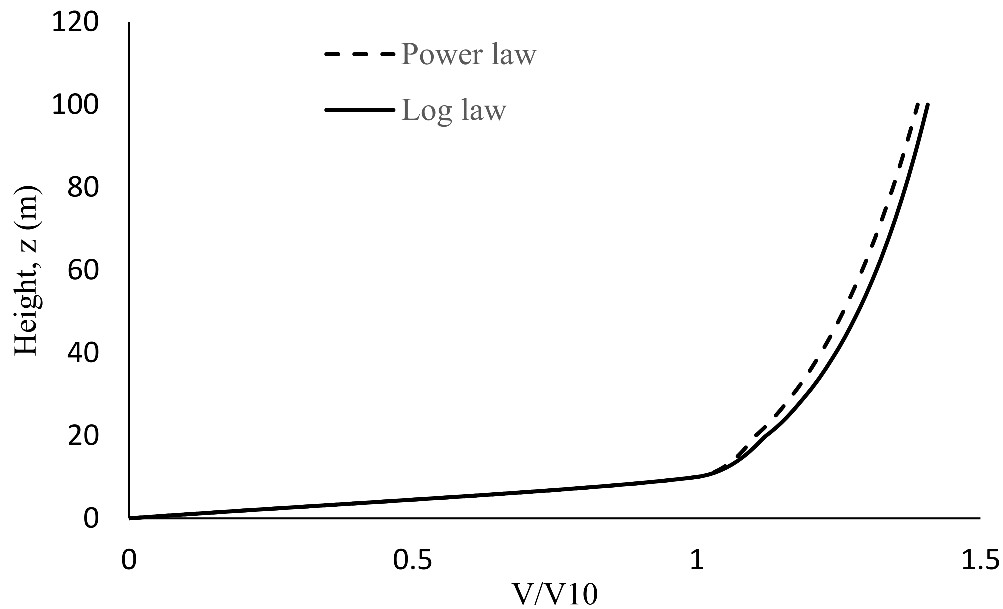

Figure 2-1: Comparison of Power law and Logarithmic law, adapted from (Holmes 2001)

The fluctuating component also known as turbulence is typified by brisk changes in time and speed. A wind spectrum is required to estimate the fluctuating component and is discussed in the next section.

2.3.3 Wind spectrum

The fluctuating component of the wind or wind turbulence is the associated fluctuation, in the instantaneous wind speed, about the mean wind speed. These fluctuations are described by a probability density function defined in the frequency domain, called the wind spectrum. It is a dimensionless number that describes the frequency of dispersion of wind at mean speed V (Zielińska and Zarychta 2015). The functions of the wind spectrum are empirically approximated based on analysis results of field experiments. Two most famous wind spectra: the Kaimal spectrum (Kaimal et al.

1972) and Davenport Spectrum (Davenport 1961) are discussed in the following sections. Kaimal spectrum is used in this research.

2.3.3.1 The Davenport Spectrum

Davenport's spectrum is the power spectral density spectrum that does not depend on height. He studied 70 spectra of horizontal gustiness of wind. The spectra were produced at different mean wind speeds, heights above the ground, and the ground roughness. The following empirical relationship was proposed for the spectrum of gustiness:

$$S_z(f) \times df = 4kV_1^2 \frac{x}{(1+x)^{\frac{4}{3}}} \times dx \tag{2.3}$$

Where $S_z(f)$ is power spectrum at height z, f is frequency, $V_1$is wind speed at standard height of 10m, k is the drag coefficient with reference to mean velocity at 10m, and x is equal to $1200f/V_1$ (where f/V_1 should be in cycles/meter), dx and df are a small change in x and f respectively.

2.3.3.2 The Kaimal Spectrum

Kaimal (Kaimal et al. 1972) conducted an experiment in 1968 in Kansas that involved measuring the wind speeds at three levels on a 105 ft. high tower. Fourier technique was employed to calculate the spectra and the following relationship was proposed by Kaimal:

$$S_{ka}(f,z) = \frac{200zu_*{}^2}{U_z(1+50\frac{zf}{U_z})} \tag{2.4}$$

Where f is the frequency in Hertz and z is the height above ground. U_z is the mean wind speed at height z and u_* is defined as shear velocity and can be expressed as:

$$u_* = \frac{U_z * \kappa}{\ln\left(\frac{z}{z_0}\right)} \tag{2.5}$$

Where U_z the velocity at height z in m/s, κ is von Karman constant roughly equal to 0.4. z is the height above ground and z_0 is terrain roughness coefficient. Higher the roughness of terrain, higher is the value of z_0. For open terrain it is roughly 0.035 m.

The advantage of Kaimal spectrum over Davenport spectrum is that it accounts the dependence of spectrum on the height of the structure above ground level.

2.3.4 Wind speed distribution

Due to high computational requirements, the simulation of wind time history for the entire year was not possible. So, a representative period of 60 seconds was selected to calculate the fatigue damage. To evaluate the damage for the entire year a wind distribution is required. It is a probability distribution function that represents the possibility of wind occurrence at certain wind speed and in a certain direction. Multiplying this probability function with the corresponding representative period would give the damage for the entire year.

Joint probability function was used to calculate the probability of occurrence of wind in a certain direction at a given mean speed. First, a basic statistical analysis was performed to calculate the individual probabilities of wind in a certain direction and speed. Then a conditional probability function was defined as the probability of occurrence of wind in a specific direction for a given mean speed. The joint probability of simultaneous occurrence of wind in certain speed and direction can be found from the formula:

$$P(S \cap D) = P(S) \times P(D/S) \tag{2.6}$$

Where $P(S \cap D)$ is the joint probability of wind at certain speed and direction, $P(S)$ is the independent probability of wind at certain speed and $P(D/S)$ is the conditional probability of wind in a certain direction for a given speed.

2.4 Weld description

Welding is the process of joining materials using high heat to melt the parts and allowing them to cool causing fusion. To add strength to the joint, in addition to the base metal, a filler alloy is also added to the joint that form a molten pool which on cooling form a rigid joint. Welding also requires some form of shielding of the welding environment to protect the molten metals from oxidation. Depending on the quality of weldment, the welded joint can be stronger than the parent metal. However, an improper welding process can introduce characteristics to the weldment like residual stresses, stress concentrations, and imperfections, which adversely effects the strength of the joint. In the present study the members of the sign structure are connected using tube to tube fillet welds. Such a fillet welded tubular joint, because of varying cross section at the joint, has non-uniform stiffness that causes stress concentration in the joint. When subjected to repeated loading cycles these joints are prone to failure due to fatigue. Presence of weld defects such as voids, residual stresses, inconsistent penetration further reduce their strength. Scanning Electron Microscopy of the failed joints performed at the Centre of Material and Sensor Characterization (CMSC) at the University of Toledo (Nims 2019) revealed that the deteriorated joints displayed characteristics of fatigue assisted crack propagation due to the presence of high concentration of spherical voids that appeared to form an interconnected network of microcracks. The extent of weld penetration was also found to be highly variable and inconsistent. Figure 2-2 and Figure 2-3 shows the various weld inconsistencies found during the study (Nims 2019).

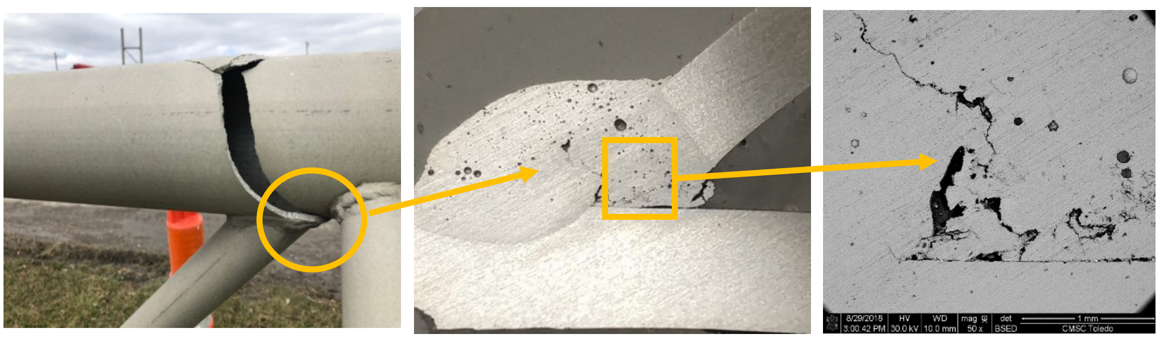

Figure 2-2 Images of weld microscopy showing spherical voids and microcracks (Nims 2019)

Figure 2-3 Images of weld microscopy showing inconsistent weld penetration (Nims 2019)

2.5 Fatigue background

Fatigue is defined as the weakening of material by the cyclic application of loads. Each cycle inflicts small amount of damage, and this damage accumulates with repetition of load cycles ultimately resulting in the failure of the structure. Typical fatigue failure surface exhibits two different cross section characteristics. A smaller smooth surface reflecting instantaneous material failure. This is the region of crack initiation. Damage during this phase is hard to quantify as this is due to microcracks that cannot be easily detected. Second zone is a much larger uneven and irregular surface due to slow material failure. This is the region where crack, after initiation, propagates slowly along the circumference until failure occurs. Damage during propagation can be quantified by measuring the length of the crack.

Stress at which fatigue damage occurs is much less than the strength of the material typically quoted as the yield strength or ultimate strength. If stresses are above a certain threshold, microcracks begin to form at locations of stress concentration and eventually a critical crack is initiated that, with repeating load cycles, gradually propagates to cause failure. If the number of cycles at a stress range before failure, in other words the fatigue life, can be accurately measured, such failures can be mitigated.

2.5.1 Fatigue strength assessment procedure

Since fatigue is a cyclic phenomenon, any fatigue assessment procedure involves comparison of the repetitive action (stress range and their frequency of occurrence) that the component or structure under consideration sustains during its life with the resistance it can offer to these actions (cycles endured before failure). This action-resistance relationship is usually expressed in terms of S-N curves. These curves relate the applied cyclic stress range (S) to the number of cycles (N) at that stress range that cause failure. To assess the fatigue life of a detail under constant amplitude stress range, number of cycles of applied stress range (n) are compared with cycles to failure (N). In the case of variable amplitude stress ranges, cumulative damage due to individual constant amplitude stress cycles is determined. This requires conversion of variable amplitude stress history into countable constant amplitude stress cycles (the process of cycle counting) and employing damage summation rule such as Palmgren-Miner rule. The location where stress in a detail is monitored, and the associated S-N curve to be used depends on the type of assessment being performed. (Maddox 2003) summarizes the following methods for fatigue assessment of welded joints.

(a) Nominal stress approach in conjunction with S-N curve for specific weld details
(b) Structural hot spot approach in conjunction with S-N curve for welds
(c) Effective notch stress approach I conjunction with S-N curves for materials
(d) Fracture mechanics approach based on fatigue crack propagation considerations

2.5.1.1 Nominal Stress Approach

Nominal stress is the stress calculated based on net cross section of the specimen. Standard strength of material equations of bending and axial stresses is used. Nominal stress in a component can be calculated with ease without any excessive error (Dexter, R.J. and Fisher 1999). S-N curves to be used in conjunction with nominal stresses are obtained from the laboratory testing of specimen containing the specific weld detail. Since the S-N curve is unique to pre-defined weld details, the quantification of stress concentration effect near the weld detail is not required. As a result, the design curves are used alongside the nominal stress range near the weld detail.

2.5.1.2 Structural hot spot approach

Hot spot stress is the stress in the structural component at the toe of weld. Hot spot stress is used in complex structures where due to non-uniform stress distribution, structural discontinuities, steep stress gradients, the definition of nominal stress is not obvious (Dexter, R.J. and Fisher 1999). It is determined by extrapolating the stress distribution approaching the weld as shown in Figure 2-4. Hot spot stress accounts for the stress concentration effect due to structural detail but ignores the local notch effect of the weld toe. This method also utilizes the resistance data based on S-N curves obtained from the experimental tests on actual weld details. However, instead of nominal stress, the S-N data is based on structural hot spot stress.

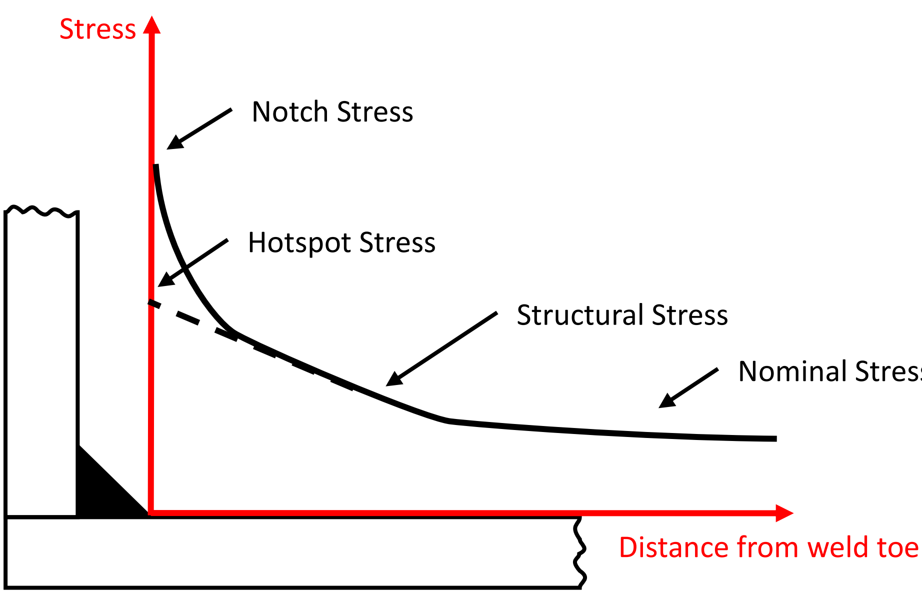

Figure 2-4: Stress profile near weld detail

2.5.1.3 Effective notch stress approach

Effective notch stress is the total stress at the weld toe considering stress concentration effects from all the factors including local notch and obtained assuming linear elastic material response. To avoid singularity due to re-entrant corners at the root of the notch, the real weld profile is replaced by an effective notch root radius of 1mm (Hobbacher 2015). Since stress concentration from all the sources is included in the available S-N curve, a single curve is enough for a given type of material. However, until very recently this method does not appear is many design specifications and availability of S-N curves based on notch stress for aluminum alloys is limited (Hobbacher 2015).

2.5.1.4 Fracture mechanics approach

This method is only applicable to the presumption that some flaw or defect (fatigue crack) have been introduced in the structure during its so far endured service life. Such flaws would be those detected by inspection or assumed flaws. Instead of representing resistance in terms of the number of cycles endured before failure (as in previous methods), this assessment procedure utilizes a crack growth rate to quantify the fatigue damage. Detailed description of this method is beyond the scope of this study and can be found in (Maddox 2003).

2.5.2 AASHTO S-N curves and fatigue classification

AASHTO support specifications recommend the use of nominal stress approach to quantify the fatigue life of the structures. For this method to be applicable the high cycle fatigue (HCF) should prevail that is the stresses should be within the elastic range and the number of cycles should be greater than 1000. Since, natural wind gusts conform to these criteria, the nominal stress approach is used in this study. An action-resistance relationship or S-N curve, for the in-question weld detail, is required for this method. S-N curve is simply a plot of a constant amplitude stress range, S, versus the cycles to failure, N. It generally consists of a negatively sloped line segment that horizontals out at a certain stress level and corresponding failure cycles. The point where the curve horizontals out (the slope becomes zero), marks the constant amplitude fatigue limit (CAFL) or fatigue threshold. CAFL represents a constant amplitude stress range below which expected fatigue failure will not occur. Analytical equation for a typical nominal stress S-N curve is given by the following equation (Dowling 1993):

$$N_f = C_f \times S_R^{-\frac{1}{m}} \tag{2.7}$$

where

N_f = number of cycles to failure;

$C_f \ and \ m$ = constants dependent on the material and connection detail; and

S_R = constant amplitude stress range.

Derivation of the constants in equation 2.7 depends heavily on experimental testing of different connection details and materials as well as their modifications to use in practical scenarios. Laboratory testing is conducted on small specimens, which are cycled to failure at various specific stress ranges. These specimens are constructed to be representative of the specific connection detail for a specific type of material. AASHTO support specifications classifies connection details into eight categories, A through ET. Examples of details relevant to highway support structures are anchor bolts and U bolts (Category D detail), column to base plate fillet weld (Category E detail), fillet welded tube to transverse plate connection (Category E' detail), fillet welded tube to tube connection (Category E' or ET detail). CAFL, for aluminum and steel, of the specified connection details in support specifications is listed in Table 2-1. Although the support specifications specify the CAFL for both steel and aluminum, it does not specify S-N curves for aluminum connection details. S-N curves for steel specified in AASHTO support specifications are depicted in Figure 2-5. AASHTO LRFD bridge design specifications (AASHTO 2012) provides S-N curves for aluminum but does not include the ET category weld detail.

Table 2-1: CAFL for AASHTO support specifications' detail categories

Fatigue Category	CAFL for Steel (MPa)	CAFL for aluminum (MPa)
A	165	70
B	110	41
B’	83	32
C	69	28
D	48	17
E	31	13
E’	18	7

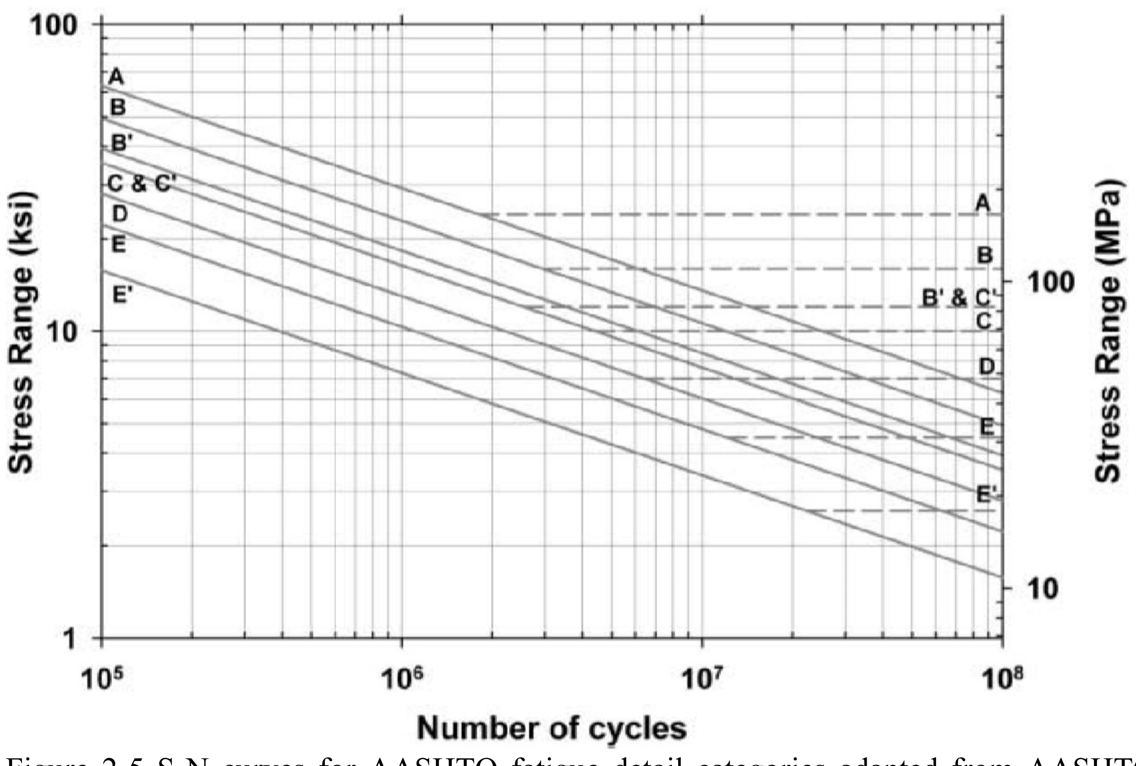

Figure 2-5 S-N curves for AASHTO fatigue detail categories adapted from AASHTO support specifications (AASHTO 2015)

2.5.3 Mean stress effect

An important consideration while using the S-N curve approach to evaluate the fatigue life is the effect of mean stress. Mean stress is defined as the average of maximum and minimum stress during a fatigue cycle. The standard S-N curve data is generated assuming a zero mean stress i.e. the load cycle is completely reversed about zero stress. The stress ratio, R is defined as the ratio of minimum and maximum stresses in the cycle and is representative of the mean stress. For a fully reversed loading (zero mean stress), the value of R is -1. Figure 2-6 shows the representation of zero mean stress.

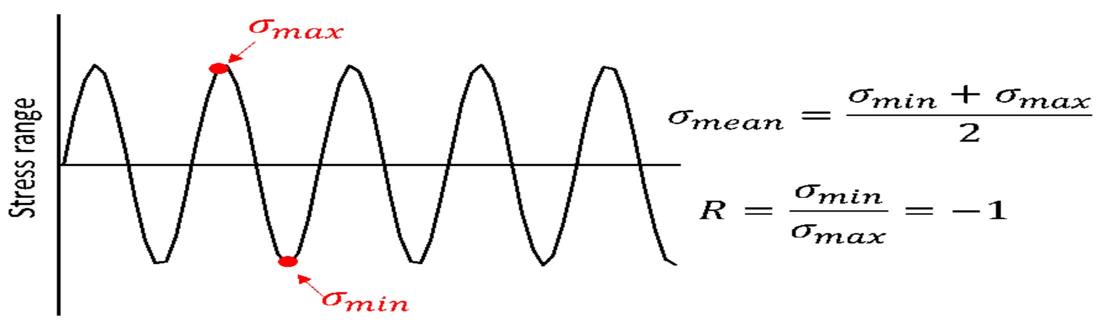

Figure 2-6: Stress cycles with zero mean stress

However, the conditions of fully reversed loading are rarely met in real engineering problems. More complex and realistic loading often results in non-zero mean stress. To account for this, a mean stress correction is applied to alternating stress. The obtained 'effective' alternating stress can then be used with zero mean stress S-N curves. Goodman (Goodman 1899) proposed the following relationship for mean stress effect:

$$\sigma_{eff} = \sigma_a \left(\frac{\sigma_u}{\sigma_u - \sigma_m} \right) \tag{2.8}$$

Where σ_{eff} is the effective alternating stress after mean stress correction, σ_a is the actual alternating stress, σ_u is the ultimate strength of the material and σ_m is the mean stress.

2.5.4 Rainflow counting algorithm

Nominal stress-based S-N curve approach described above is based on constant amplitude loading events. However, due to varying nature of wind, sign structures are subjected to loading cycles of variable amplitude. Therefore, it is necessary to convert this complex variable amplitude stress history into a series of constant amplitude load events. Cycle counting is the process employed to convert complex stress histories into simpler usable form. Several counting methods such as reservoir method, peak count method, rainflow count method can be used for this purpose. Of all the counting methods available, rainflow is the most popular because of the simplicity of its algorithm, and therefore is used in this study.

The rainflow counting algorithm was first developed in Japan in 1968 and was later adopted by American Society of Testing and Materials (ASTM) (Bannantine et al. 1990). Its name comes from the analogy that when rotated by 90 degrees, the stress-time response looks like a "pagoda" roof and the cycle count could be envisioned as raindrops falling from the roof. In this study the MATLAB toolbox developed by A. Neislony (Nieslony 2009) was used to convert stress time histories into number of cycles of variable stress ranges.

2.5.5 Palmgren-Miner rule

When a structure is subjected to varying stress ranges that cause different degree of damage to the structure, a damage summing method is required to predict the fatigue life of the structure. Palmgren-Miner rule is a widely accepted rule to predict the fatigue life of varying-amplitude loading. Proposed by Palmgren in 1924 and developed by Miner in 1945 (Bannantine et al. 1990), the procedure assumes that the damage contribution of any particular stress range is a linear function of the number of cycles experienced by the structure at that stress range. Linear addition of the damage contribution from all the stress ranges that are applied on the structure gives the accumulated damage. Failure occurs when the accumulated damage reaches unity.

If D_i is the damage fraction due to a stress range of S_i, n_i is the number of stress cycles at this stress range and D is the total damage factor then:

$$D_{\mathrm{i}} = \frac{n_i}{N_i} \tag{2.9}$$

$$D = \sum D_i \tag{2.10}$$

where N_i is the number of cycles to failure at stress range S_I and can be found from the S-N curve.

Although this method may be useful in many circumstances, it has certain limitations. The most common limitation is its failure to account for the sequence effect of stress ranges. It assumes that every cycle is a stress range causes equal damage independent of the effects of previous stress ranges. However, in certain circumstances, low-stress cycles followed by high-stress cycles are found to cause more damage than predicted by the rule (Eskandari and Kim 2017). Also, the procedure is independent of the average stress in the cycle. However, when analysis is limited to the elastic region only (as is the case in the present study), it is found that these factors have very little influence on the results (Bannantine et al. 1990). AASHTO also specifies the use of Miner's rule to calculate accumulated damage.

Chapter 3

Structural analysis

3.1 Description of Truss

The investigated truss is located at Alum Creek drive, Columbus, Ohio. The coordinates of the site are 39°52'11.4"N 82°56'03.2"W. A google satellite view of the truss is shown in Figure 3-1.

Figure 3-1: Satellite image adopted from google

The truss is a three-dimensional space frame having a span of 90 feet. Truss was mounted over the steel supports using U-bolts at a height of 23 feet from the ground. Four parallel aluminum chords run along a 4ft by 4ft grid to which aluminum diagonals are welded at equal intervals. The chords of the truss are circular hollow tubes having outer and inner diameters as 4.8125” and 4.3750” respectively. The diagonals are also hollow pipes having 1.9375” and 1.5625” as outer and inner diameters respectively. After the failure was observed, truss was dismantled and is shown in Figure 3-2.

Figure 3-2: Dismantled truss

The truss was erected in 1996. In the beginning, two traffic signs of size 12’×7.5’ and 13’×5.5’ were mounted by 3-Z bar assemblies. These signs were later replaced by smaller signs of size 5’×3’. A schematic diagram of old and new sign dimensions and their mounted position is shown in Figure 3-3.

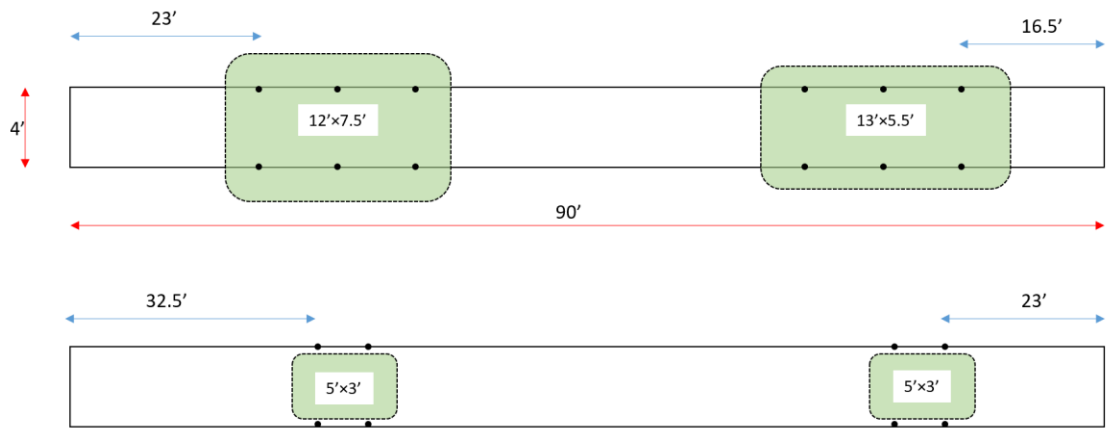

Figure 3-3: Schematic diagram of old and new sign boards respectively

3.2 Visual inspection

A team of professors along with ODOT inspectors visited the site of failed truss to examine the cracks and determine possible failure causes. Circumferential fractures were observed at two adjacent locations on one end of the truss, at the weld junction of diagonals and chord. Visual inspection of the fracture surface exhibited two different cross section characteristics. A smaller smooth surface reflecting instantaneous material failure. This is the region of crack initiation. A much larger uneven and irregular surface due to slow material failure. This is the region where crack, after initiation, propagated slowly along the circumference until failure occurred. This type of fracture surface exhibits a typical fatigue failure and is depicted in Figure 3-4. However, there are several other factors that can augment this rupture such as overloading, heat-zone effects, corrosion, weld defect etc. Samples of good and bad regions were cut and retrieved to the university for material testing.


Figure 3-4: Fractured chord

3.3 SAP2000 modelling

As the first step in the investigation, a finite element model of the aluminum truss is developed using commercially available SAP2000. Structure is modelled as 3D space frame having a longitudinal span of 90 feet with chords spaced at four feet in both the lateral directions. Truss members are modelled using 2 node continuous beam elements whereas the sign boards are four node area elements. The small deformations due to wind loading were assumed to cause elastic response. The welds between diagonals and chord were modeled as fixed whereas the U-bold connections were kept pinned. Appropriate section and material properties were assigned to all the components of the structure. Material properties required for the linear elastic model are Young modulus, Poison's ratio, and material density. Sectional and material properties used in the model are shown in Table 3-1. These properties were acquired from the drawings provided by the ODOT and verified from field measurements. A geometry of the model with bigger sign boards along with boundary conditions is shown in Figure 3-5.

Table 3-1: Section properties and material properties

Component	Material	Outside diameter	Wall thickness	Yield strength (ksi)	Young's Modulus (ksi)
Truss members					
Chord	Aluminum	5.50"	0.250"	35	10100
Vertical diagonal	Aluminum	1.90"	0.145"	35	10100
Horizontal and Internal diagonal	Aluminum	2.00"	0.188"	35	10100
Support structure					
Column	Steel	8.00"	0.889"	50	29000
Bracing	Steel	2.37"	0.154"	50	29000
Split-tee	Steel	WT4"X6.5"		50	29000

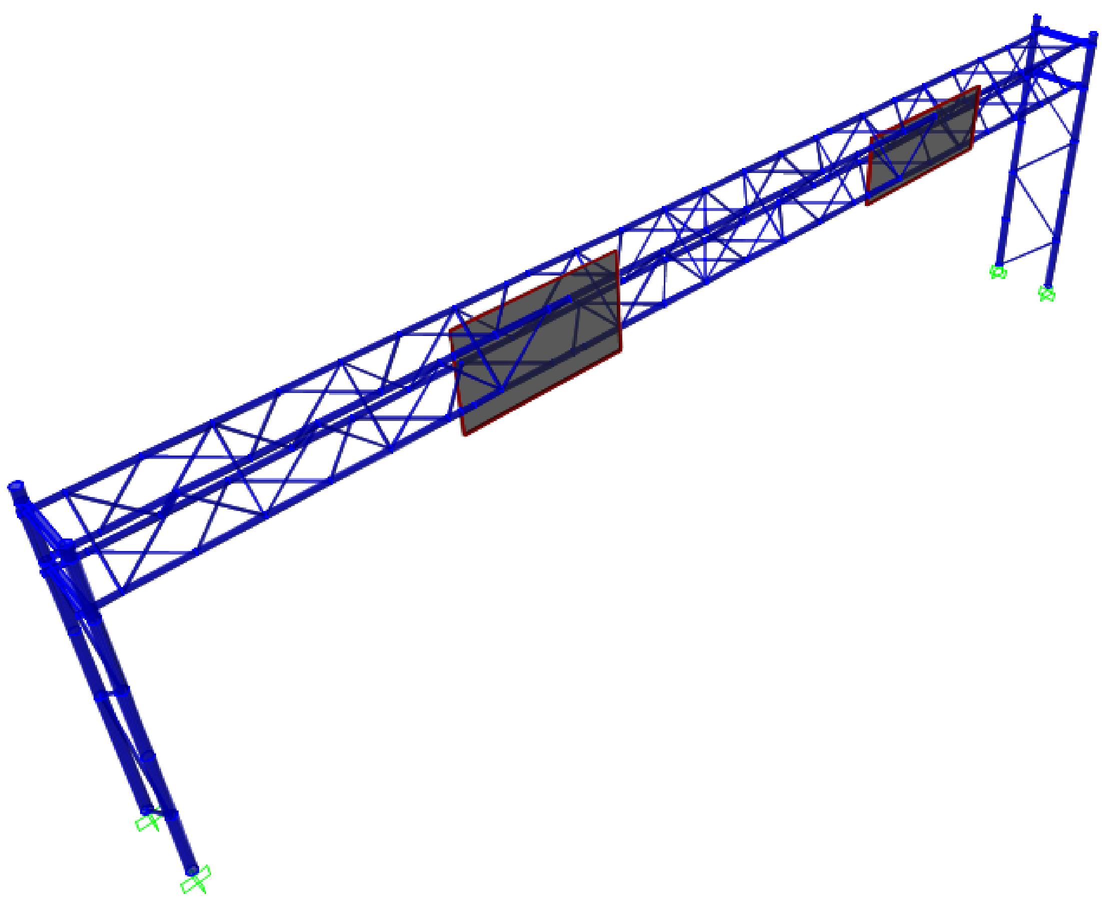

Figure 3-5 Finite element model of the truss along with boundary conditions

Once the model was generated, following types of linear elastic analysis were performed. The results from each analysis are presented in the subsequent sections.

1. Modal analysis
2. Linear static analysis under equivalent static wind loads and gravity loads
3. Linear static analysis under equivalent static pressure range (fatigue)

3.3.1 Modal analysis

Dynamic characteristics of a structure are greatly influenced by its support conditions. Therefore, a modal analysis was performed to evaluate the dynamic behavior of the model given varying support conditions. The two support conditions used in the modal analyses were "fixed" base and "pinned" base. First four mode shapes for fixed base are shown in Figure 3-6.

Mode 1: This is the longitudinal motion of the truss developed entirely due to the deformation of supports. It is excited by the loads acting across the load and longitudinal to the span of the truss. Due to the slim profile of truss in this direction, it is difficult to excite this mode, to any considerable extent, due to wind gusts.

Mode 2: This is the horizontal motion of the truss in the direction of the road. It is excited by loads perpendicular to the span of the truss. Major portion of wind gust on sign boards and truss profile acts perpendicular to span, therefore this mode is most easily excited.

Mode 3: This is the vertical motion of the truss caused due to a combination of bending of truss and support columns. Component of wind gust acting perpendicularly upwards or downwards to roadway can excite this mode.

Mode 4: This is the twisting motion of the truss and supports under wind load. This mode has a considerably higher frequency of vibration than the first three modes.

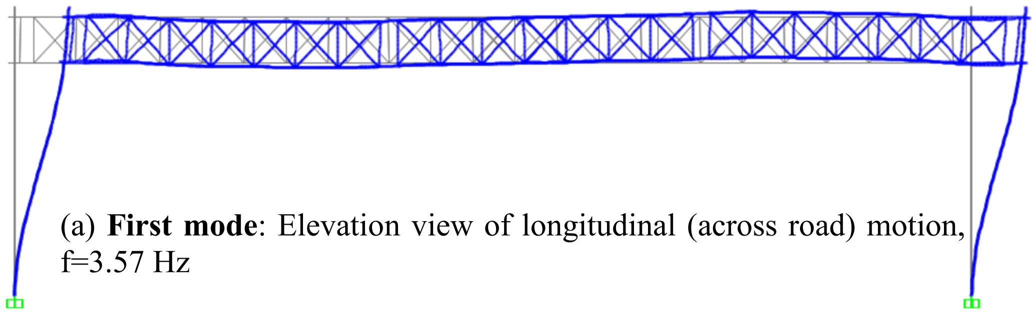

(a) **First mode**: Elevation view of longitudinal (across road) motion, f=3.57 Hz

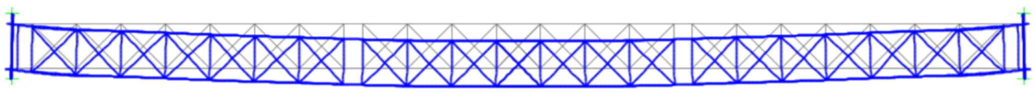

(b) **Second mode**: Plan view of horizontal (along road) motion, f=4.59

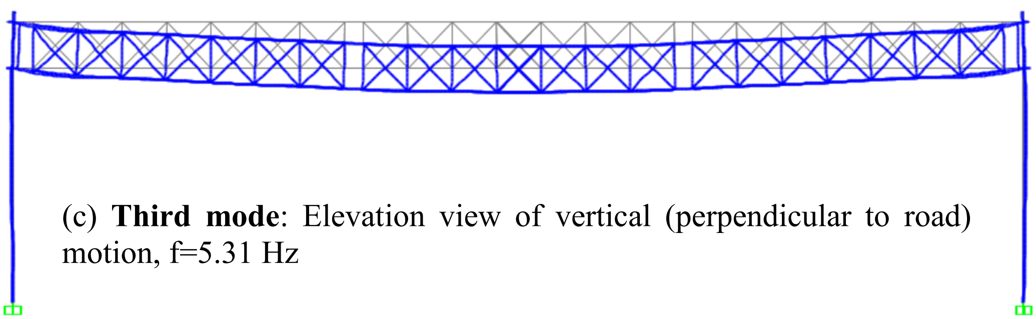

(c) **Third mode**: Elevation view of vertical (perpendicular to road) motion, f=5.31 Hz

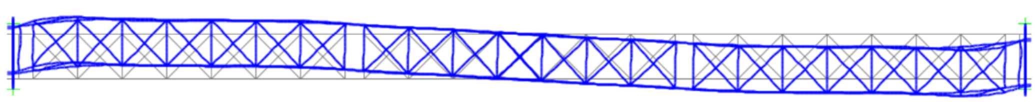

(d) **Fourth mode**: Plan view of twisting motion, f=11.31 Hz

Figure 3-6:(a) to (d)- First four mode shapes for fixed base case

Table 3-2 show the comparison of natural frequencies, for the first 10 modes, found in fixed and pinned base case. It is evident from Table 3-2 that natural frequencies in modes two through five are almost the same for the two cases and support conditions contribute little to the dynamic behavior of the structure. Effect of support conditions in higher modes can be ignored as these modes will not be excited in the current analysis. It is a valid assumption as the wind loading used in the subsequent analyses is generated using Kaimal spectrum, which employs frequencies of less than 10 Hz to account for the wind turbulence. The large variation in frequency of vibration of mode 1 lies in the fact that this mode is governed by the lateral sway vibration of the support columns and is, therefore, directly affected by the support conditions. However, as mentioned above, to excite this mode structure need to be loaded with a loading that is longitudinal to the span of the structure. It is possible that some component of the wind gusts acts parallel to the longitudinal chords of the truss to excite this mode, but the available surface area for such a loading would be extremely small to cause any damaging stress cycles in the structure.

The above discussion highlights the fact that the support conditions at the base have little influence on the dynamic behavior of the structure as applicable to this study. Therefore, the bottom of the structure was modeled as fixed for all the subsequent analyses.

Table 3-2: Frequency of vibration form modal analysis assuming "fixed" and "pinned" base conditions

Vibration mode	**Frequency of vibration (Hz)**	
	Fixed base	**Pinned base**
1	3.57	1.67
2	4.59	4.41
3	5.31	5.11
4	11.31	11.03
5	11.72	11.71
6	13.42	12.98
7	13.76	13.27
8	16.36	14.07
9	19.25	14.46
10	20.73	15.23

3.3.2 Static wind analysis

Equivalent static wind loads were calculated in accordance with AASHTO-LRFD 2015 to be applied on the truss. Code proposes the following equation to calculate the wind pressure.

$$q_h = 0.00256 \times K_z \times K_d \times G \times V^2 \times C_d \;\; (psf) \tag{7.1}$$

Where K_z is height and exposure whose value is 0.92 for a height of 23 ft and exposure condtion C as applicable for this truss. K_d is wind directionality factor whose value is 0.85 for overhead trusses. G is the gust effect factor equal to 1.14. V is basic wind speed at the location and is equal to 110 mph for Columbus. C_d is the drag coefficient that depends on the geometry of the member and is calculated to be equal to 1.19 for solid sign boards and 1.20 for tubular trusses.

The pressure calculated from the above equation is converted into distributed load by multiplying it by the diameter of the members. However, it is applied as pressure to sign boards. A summary of wind load applied on different components of the structure is presented in Table 3-3.

Table 3-3: Static Wind load on truss

Component	**Wind load**
Sign (uniform pressure)	1.58 kN/m^2
Chord (UDL)	0.195 kN/m
Diagonal (UDL)	0.078 kN/m

Wind loads calculated above were applied to the structure in addition to gravity loads due to self weight of structure and sign bords. Load combination of (0.9D + 1.0W) was employed and a static linear analysis was performed. The results from the analysis were examined to determine the maximum stresses in the truss and to identify the critical members. Since the members are subjected to both the axial and bending actions, the maximum stresses in the members can be calculated by superimposing the stresses from individual actions, as described below:

$$\sigma = \frac{P}{A} \pm \frac{M}{Z} \tag{7.2}$$

Where σ = Total stress in the member

M = Bending Moment

P = Axial force

A = cross-section area

Z = section modulus about axis of bending

As expected the maximum stresses were found to occur at the end of the truss. Major contribution was from axial stresses due to truss action Based on the location of highly stressed joints and failue locations, select members were identifies as critical and are shown in Figure 3-7. Chord members at failure locations have four times less stress than the chord members opposite to them. Moreover chord members have higher CAFL than diagonal members, and are less fatigue succeptible. Therefore they were excluded from the list of critical memebers. Results for these critical members are presented in Table 3-4. The chord member C329 experiances the highest stress, however it is below the allowable stress for welded Aluminum.

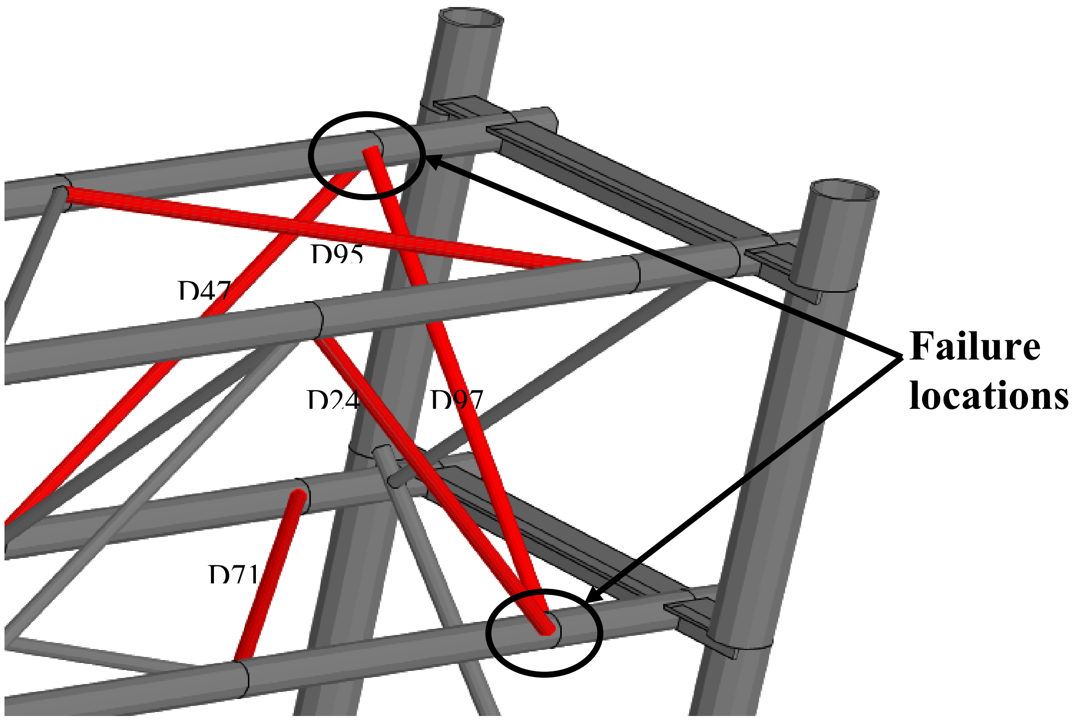

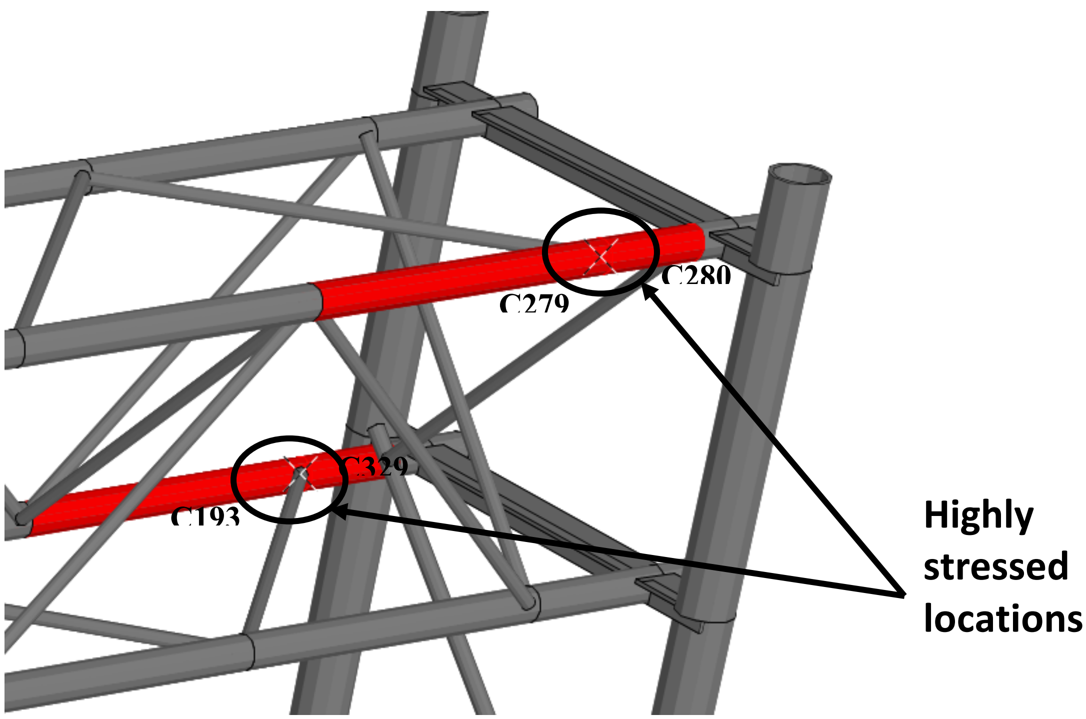

Figure 3-7: Critical chord and diagonal members

Table 3-4: Stresses in critical members for design wind and gravity loads

Member	Stress (Small sign) (ksi)	Stress (Large sign) (ksi)	% Reduction
C329	5.3	11.9	55
C193	5.2	11.7	55
C280	4.6	10.5	56
C279	3.9	8.9	56
D71	5.3	11.8	55
D95	4.8	11.0	56
D24	1.7	3.9	56
D47	1.9	4.3	56
D97	1.8	4.1	56

Size of the sign board have considerable effect on the miximum stresses experianced by the structure. Replacing the older bigger sign boards (sign area = 160 ft^2) with smaller ones (sign area = 30 ft^2)- a reduction of around 80% is sign area- reduced the maximum stresses by 55%.

3.3.3 Static fatigue analysis

The AASHTO fatigue design specifications are based on NCHRP Report 412 (Kaczinski 1998). The components of a sign structure should be designed for fatigue to resist equivalent static loading due to natural wind gusts, galloping, vortex shedding and truck-induced gusts. For infinite life, the stresses should not be greater than the constant amplitude fatigue threshold (CAFL) listed for each detail category identified in AASHTO-2015. The CAFL values applicable to truss details considered in this structure are listed in Table 3-5.

Table 3-5: CAFL for different component details as per AASHTO-LTS

Component	Detail category	CAFL (ksi)
Chord	E	1.9
Diagonal	ET	0.44

Since only the vibrations caused by natural wind gust are being considered in this study, equivalent static fatigue load due to natural wind gusts only was applied to the structure. AASHTO requires the structure to be designed to resist an equivalent static natural wind gust pressure range of:

$$P_{NW} = 5.2 \times C_d \times I_f \; (psf) \tag{7.3}$$

where:

I_f = fatigue importance factor (1.0 for fatigue category 1)

5.2 = pressure (psf)

C_d = the appropriate drag coefficient based on the yearly mean wind velocity of 11.2 mph

The pressure range is applied as uniform pressure on sign boards and as distributed load on truss members. Table 3-6 shows the magnitde of load ranges applied to different components of the truss. Stresses obtained as a result of applied pressure ranges in the critical members are presented in Table 3-7. Chord members are found to have stresses that are lesser than the CAFL for category E, whereas all the diagonals members see higher stresses than allowed by the code.

Although diagonal members exceed the codal limit for fatigue, it is expected as the design of the truss is in accordance to AASHO specifications for the design and construction of structural supports for highway signs, 1961 (AASHO 1961). The fatigue design criteria were almost non-existant at that time. Also the coefficient of drag used to calculate the pressure is based on yearly mean velocity of 11.2 mph which is conservative for Columbus region that has an annual average wind velocity of 8.3 mph.

To accurately assess the fatigue performance of the structure, detailed fatigue life evaluation based on wind load history generated from past wind data is carried out and is discussed in the next chapter.

Table 3-6: Load range applied to truss members and sign boards

Component	Wind load
Sign board	5.72 psf
Chord	2.26 plf
Diagonal	0.90 plf

Table 3-7: Stresses in members from pressure range due to natural wind gust

Member	Stress (ksi)	Detail Category	CAFL (ksi)
C329	1.65	E	1.9
C193	1.65	E	1.9
C280	1.60	E	1.9
C279	1.60	E	1.9
D71	1.65	ET	0.44
D95	1.61	ET	0.44
D24	0.65	ET	0.44
D47	0.61	ET	0.44
D97	0.58	ET	0.44

Chapter 4

Fatigue analysis

4.1 Fatigue life evaluation

Analytical procedure performed to obtain estimated fatigue life of critical details is described here. Following steps were performed to calculate the accumulated damage of the members and their expected life.

4.1.1 Distribution of wind

Data for 10 years of daily wind speed and directions were obtained from the National Climatic Data Centre (NCDC). Wind data were clustered into 5 mph bins varying from 0-30 mph wind speeds. This range was selected based on the analysis of daily average wind data collected from NCDC. The frequency of occurrence of wind speeds in Columbus based on the data from the past 10 years is shown in Table 4-1.

The probability of occurrence of wind speeds higher than 30 mph is less than 0.1% and would be responsible for very few numbers of stress cycles, therefore they were excluded from the spectrum of wind distribution. Similarly, the directions of wind flow were also divided into eight bins of 45 degrees each, corresponding to four cardinal and four inter-cardinal directions. The resulting histograms of wind speed and direction distribution are shown in Figure 4-1 and Figure 4-2 respectively.

Table 4-1: Probability of occurrence of various mean speeds

Speed (mph)	No. of occurrences	Probability of occurrence
5	98015	38.15%
10	102666	39.96%
15	36852	14.34%
20	13474	5.24%
25	4817	1.87%
30	856	0.33%
35	173	0.07%
40	40	0.02%
45	11	0.00%
50	1	0.00%
55	2	0.00%

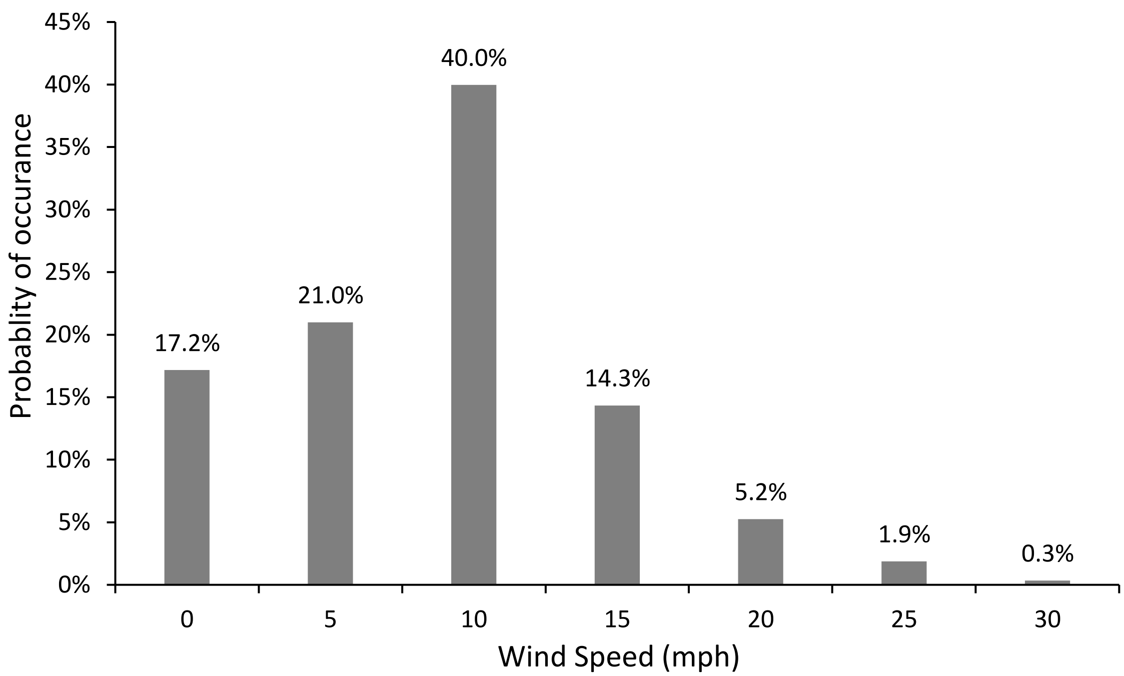

Figure 4-1: Probability distribution of wind speeds

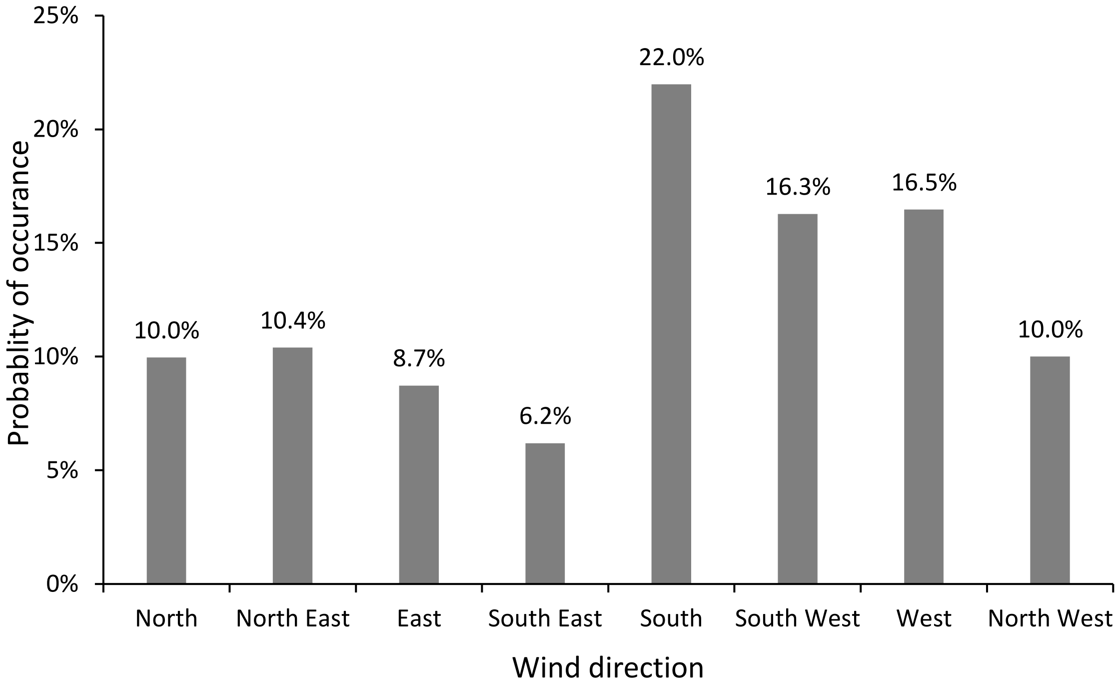

Figure 4-2 Probability distribution of wind directions

A basic statistical analysis was performed to calculate the probability of occurrence of a specific speed and direction. Joint probability function was used to calculate the direction for a given speed of the wind and is shown in Table 4-2. Since in the field, the structure was oriented in East-West direction, only the wind speeds having components in either north or south directions would hit the structure. North and South cardinal wind would hit the truss face front and therefore a 100% contribution of these probabilities is considered. However, the wind flowing in sub-cardinal directions would hit the truss at an angle and therefore only 50% contribution to fatigue damage is considered from these wind speeds. Wind speeds in the direction of cardinal Ease and West are assumed to have a negligible effect on the truss as the area of the structure perpendicular to these directions are minimal.

Table 4-2 Joint probability distribution of wind speed and direction

		Wind speed (mph)					
		5	**10**	**15**	**20**	**25**	**30**
Wind Direction	**N**	1.61%	4.15%	1.80%	0.53%	0.10%	0.01%
	NE	2.82%	5.00%	1.01%	0.21%	0.04%	0.00%
	E	2.86%	4.22%	0.75%	0.09%	0.01%	0.00%
	SE	2.30%	2.97%	0.39%	0.10%	0.02%	0.00%
	S	5.16%	9.08%	3.06%	0.92%	0.28%	0.04%
	SW	2.98%	5.85%	2.40%	1.16%	0.54%	0.12%
	W	1.74%	4.96%	3.15%	1.60%	0.69%	0.14%
	NW	1.52%	3.74%	1.78%	0.64%	0.19%	0.02%

4.1.2 Wind load time history

As discussed in section 2.3.4, it is computationally very expansive to model transient wind load for the entire year. So, a representative time that is long enough to satisfactorily capture the fluctuating nature of wind need to be established. A wind spectrum assumes that over a period the statistical characteristics of wind can be regarded as constant. To further verify this assumption instantaneous wind velocities for durations of time varying from five seconds to one hour were generated and statistically compared. Figure 4-3 displays the instantaneous wind velocities for different periods of time sampled at 10 Hz. Mean and standard deviation of the different plots is shown in **Error! Reference source not found.**. From table, it is evident that the statistical variations of wind velocity are independent of the duration of time for which it is generated.

Table 4-3 Statistical comparison of wind speeds generated for different periods of time

Time duration (seconds)	Mean	Standard deviation
5	4.25	0.33
60	4.24	0.32
600	4.24	0.32
3600	4.25	0.32

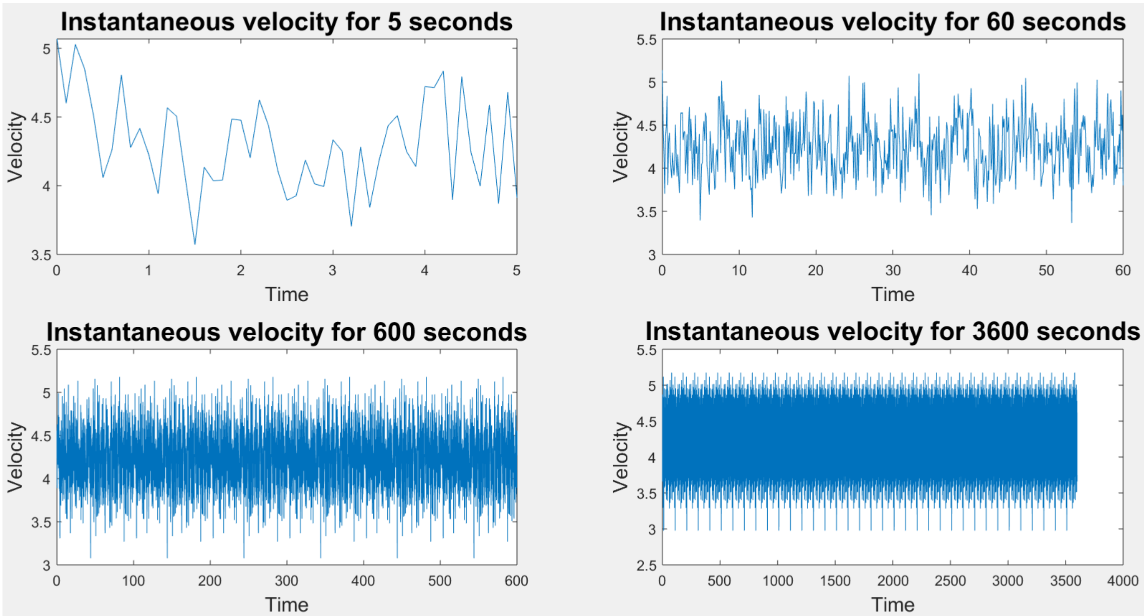

Figure 4-3: Wind velocities for various representative times

Also, once the representative time was established, it was important to verify the frequency content of the generated wind velocity profile. In section 3.3.1 it was assumed that frequency modes higher than 10 Hz would not be excited in the present study. So, it is necessary that the frequency content of the generated wind profile is within the assumed limits. The wind profile for 60 second period was passed through a Fast Fourier Transform (FFT) and the plot is displayed in Figure 4-4. It is evident from the figure that the no frequency content of the wind velocity is greater than 5 Hz. Therefore, the generated wind velocity profile could be safely used to model the wind load on the structure.

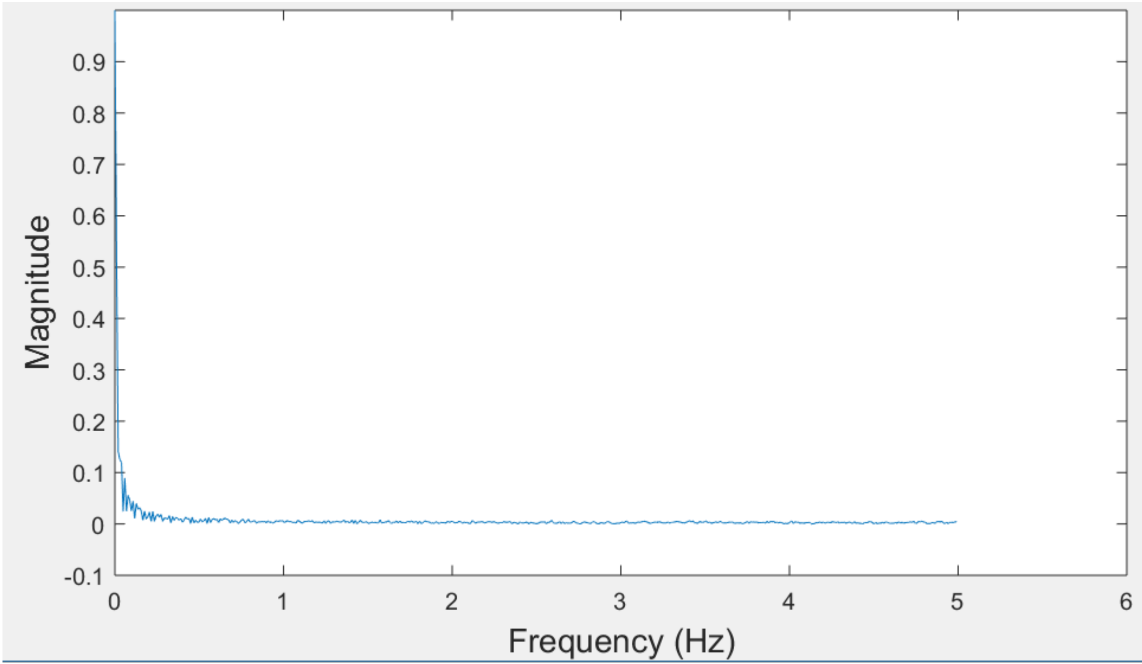

Figure 4-4 Plot of Fast Fourier Transform of 60 second wind velocity

A representative period of 60 seconds was selected to develop the transient wind load history to be applied to the structure. The effect of a given duration of time can be evaluated by multiplying the effect of 60 second period by the number of 60 second periods occurring in the given time. The scope was to model the turbulent nature of the wind in horizontal direction. As discussed earlier, the instantaneous wind speed can be considered as a resultant of two components: a mean component V and a fluctuating component $v'(t)$. Wind speeds ranging from 5mph to 30mph at an interval of 5 mph were used. Mean component V of wind at the height of the truss (23 ft) was calculated using the power law. The fluctuating component $v'(t)$ can be found by using either Constant Amplitude Wave Superposition (CAWS) or Weighted Amplitude Wave Superposition (WAWS) (Iannuzzi et al. 1987). WAWS method is used in this research and it gives the following equation to calculate the fluctuating component:

$$v'(t) = \sum_{k=1}^{N} \sqrt{2S_{ka} f_k \Delta f} \times \cos(2\pi f_k t + \phi_k) \tag{8.1}$$

Where $v'(t)$is the fluctuating component of wind, f_k is the frequency at time t, S_{ka} is the Kaimal spectrum constant, Δf is the frequency increment, ϕ_k is the phase angle distributed randomly between 0 and 2π, and N is the total number of time increments.

After summing the two components, the wind pressure P(t) to be applied on the structure can be calculated as:

$$P(t) = \frac{1}{2} \rho C_d V(t) \tag{8.2}$$

where $V(t)$ is the instantaneous velocity (sum of mean and fluctuating components), ρ is the air density, and C_d is the coefficient of drag.

A MATLAB script, to implement the above procedure, was written and is included in the Appendix. The flowchart of the MATLAB program is shown in Figure 4-6. It generated wind pressure as a function of time at various mean wind speeds which was then read into the SAP2000 as a transient load. Figure 4-5 shows the plot of wind pressure versus time for various wind speeds.

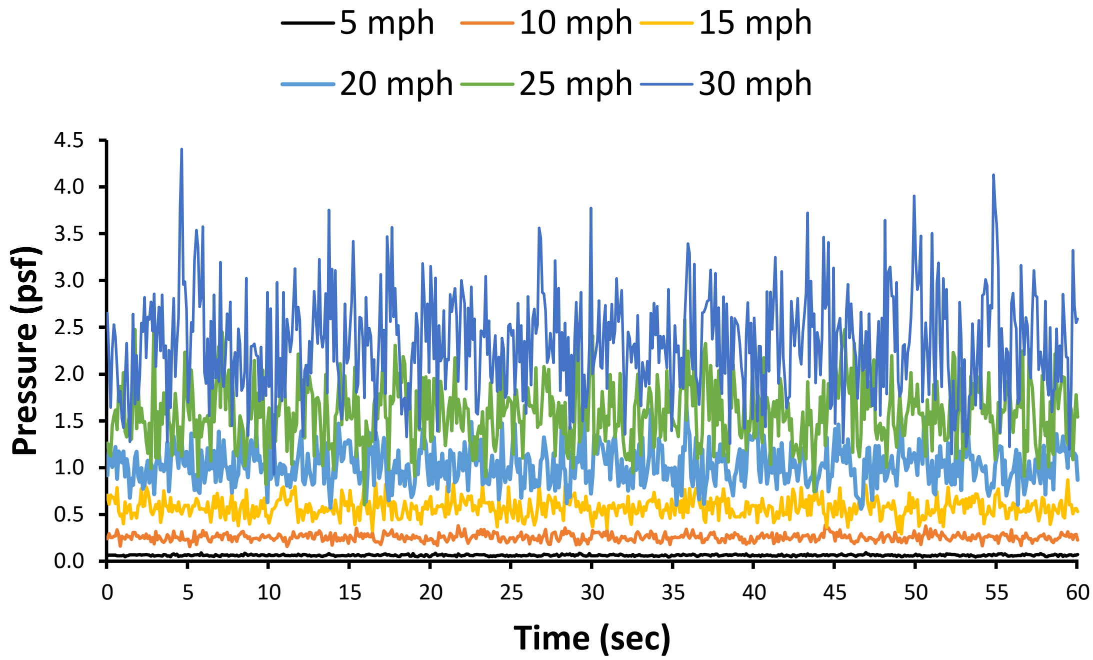

Figure 4-5: Wind pressure for 60 second period at various mean wind speeds

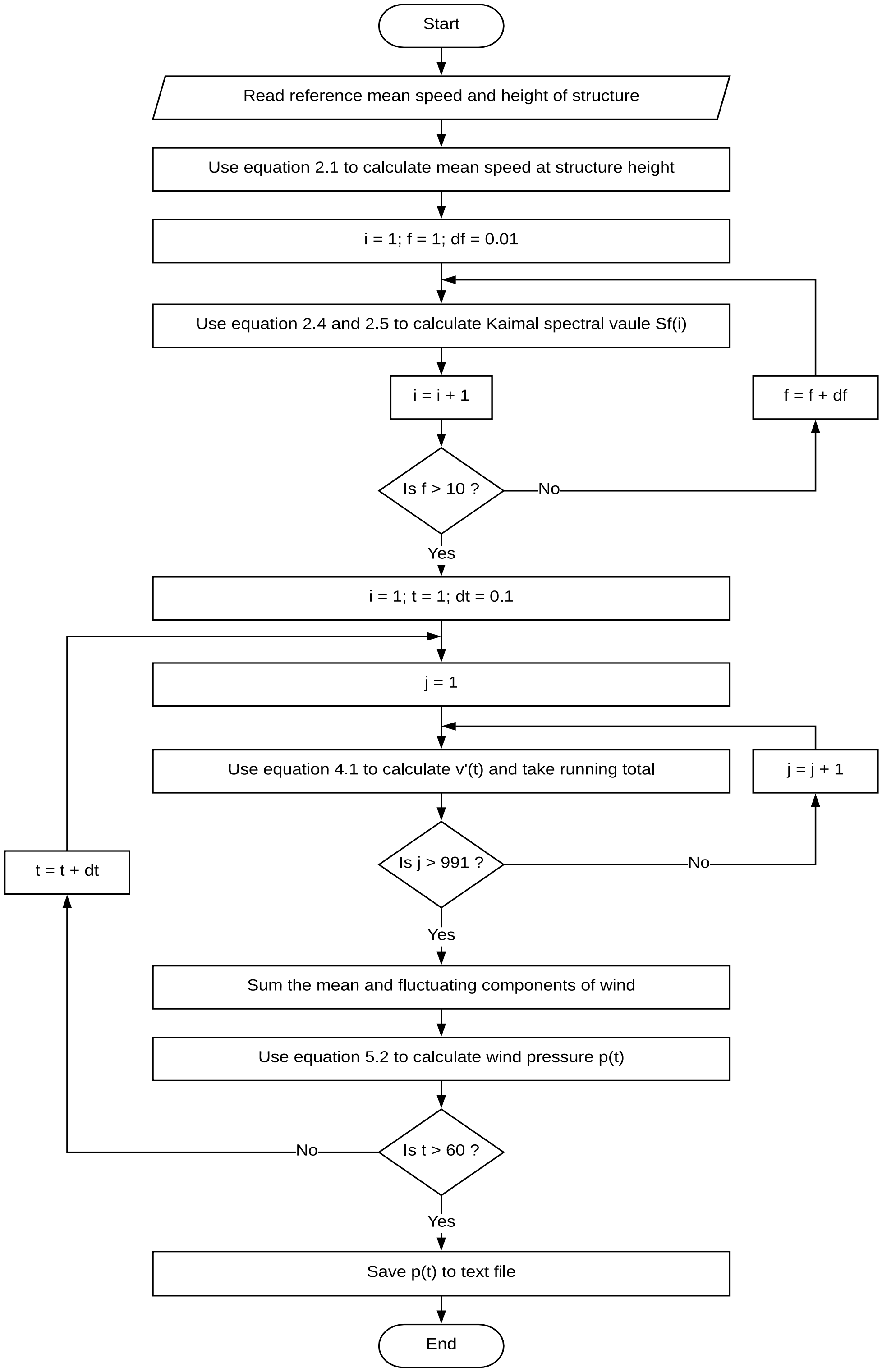

Figure 4-6: Flowchart of MATLAB program for wind time history

4.1.3 Nominal stress history

Once the pressure generated in the above step was applied to the structure and analysis was performed, stress history of any member for 60 second period can be extracted from the results of the analysis. Nominal stress assessment requires establishing a reference point on the member where stress is not affected by weld detail and investigating the stress distribution adjacent to weld detail. Nominal stress at the weld detail is then calculated based on reference stress and slope of the stress distribution away from the weld detail. However, if the stress distribution along the member is uniform as is the case in a tubular truss, nominal stress is the same as reference stress. Also, a “stick model” (like SAP2000) does not account for stress variations due to weld detail, so any value of maximum sectional stress near the weld detail would give the required nominal stresses. Nominal stress history for 60 second period at various mean speeds was extracted for all the critical members. This obtained nominal stresses are then amplified using Goodman relation (equation 2.7) to account for mean stress effect. Figure 4-7 represents the nominal stress history of Member 95 (see Figure 3-7).

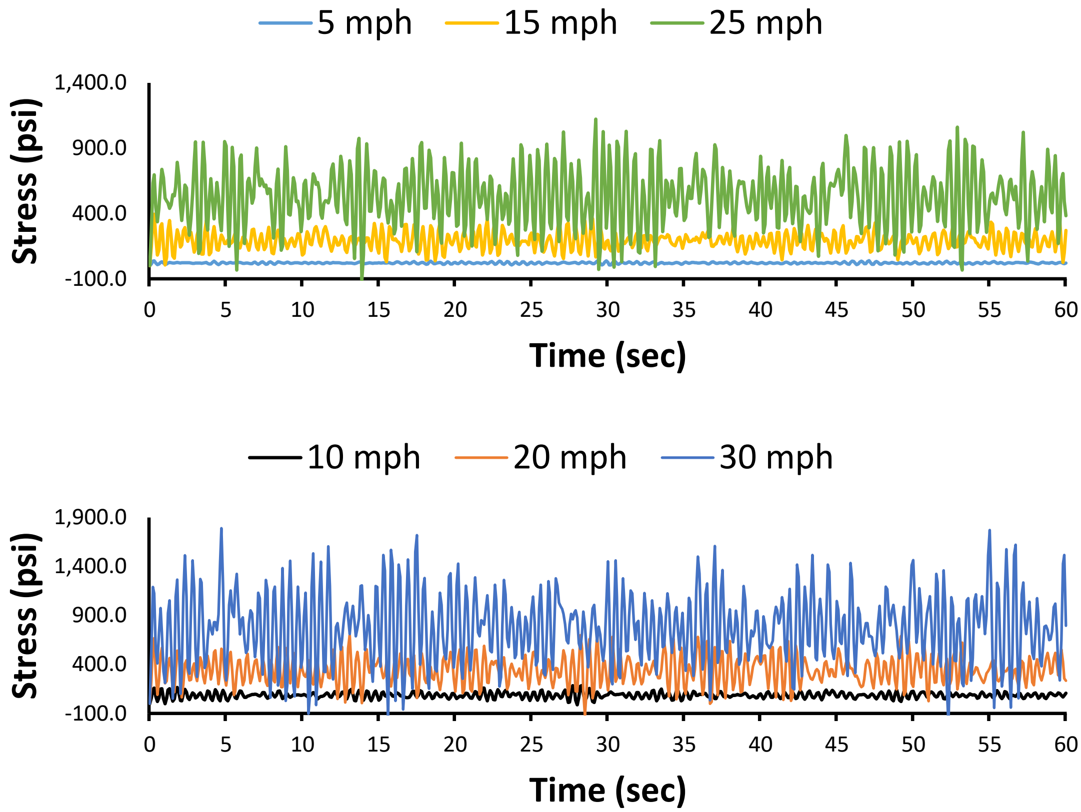

Figure 4-7: Nominal stress history for 60 second period of Member 95

4.1.4 Damage calculation and Life estimation

As described in section 2.5.4, the obtained variable amplitude stress history needs to be converted into constant amplitude stress events before fatigue life can be evaluated. Rainflow counting algorithm is used for this purpose. Mat-lab script developed by (Nieslony 2009) and available to download on MathWorks website (https://www.mathworks.com/matlabcentral/fileexchange/3026-rainflow-%counting-algorithm) was used to count the number of cycles in variable amplitude stress history. The input for the script is a text file containing the stress time history of individual members. The rainflow algorithm reads a history of peaks and valleys of stress data, in sequence, and groups together the stress cycles of similar magnitude. The output is a histogram of the count of cycles of different magnitude.

Once the variable amplitude stress history is broken down into a series of constant amplitude stress events. Miner's rule is applied to calculate the accumulated damage from these stress ranges.

The damage fraction D_i due to a stress range of S_i is given by:

$$D_i = \frac{n_i}{N_i} \tag{8.3}$$

$$D = \sum D_i \tag{8.4}$$

Where n_i is the number of stress cycles at the stress range S_i (obtained from rainflow counting) and N_i is the number of cycles to failure at stress range S_i (can be found from above equation). The total damage is found by summing the individual damage from every cycle. The total damage caused by the 60-second wind load for various mean wind speeds in critical members is shown in the table below:

Table 4-4: Damage factor for 60 second wind load

Wind speed	**Damage factor D_i**				
	Member 24	**Member 47**	**Member 71**	**Member 95**	**Member 97**
5	1.3E-12	9.2E-13	2.1E-11	3.2E-11	1.1E-12
10	1.3E-10	8.9E-11	2.1E-09	3.2E-09	1.1E-10
15	1.8E-09	1.3E-09	3.1E-08	4.6E-08	1.6E-09
20	1.2E-08	8.4E-09	1.9E-07	3.0E-07	1.1E-08
25	5.0E-08	3.8E-08	8.5E-07	1.3E-06	4.5E-08
30	1.9E-07	1.4E-07	3.2E-06	4.8E-06	1.7E-07
Sum	**2.5E-07**	**1.9E-07**	**4.2E-06**	**6.4E-06**	**2.3E-07**

Because the load on the model, was applied only for a 60 second period, the number of such periods over one year (525600) was found. Also, since the structure is oriented in

East-West direction in the field, only the wind speeds having components in North-South directions would cause damage in the structure. So, the number of 60 seconds time periods in one year was multiplied by the probabilities associated with the appropriate directions as described in section 4.1.1, to give the effective number of 60 second periods per year experienced by the structure and is shown in Table 4-5 below.

Table 4-5: Number of effective 60 second periods for various mean wind speeds

Wind speed	**Effective 60s periods/year**
5	60194
10	115507
15	39310
20	12709
25	3919
30	595

Finally, the damage caused in one year is found by multiplying the summed damage at a specific wind speed by the number of effective 60 second periods/year of the corresponding wind speed. The life expectancy of the member can be calculated by dividing the total damage by one and is shown in Table 4-6. The horizontal diagonal at the top is found to be most critical with an expected fatigue life of 72 years which exceeds the expected service life of the truss (typically 50 years).

Table 4-6: Yearly damage for various wind speeds and expected life of critical members

Wind speed	**Total damage**				
	Member 24	**Member 47**	**Member 71**	**Member 95**	**Member 97**
5	7.6E-08	5.5E-08	1.3E-06	1.9E-06	6.8E-08
10	1.5E-05	1.0E-05	2.4E-04	3.7E-04	1.3E-05
15	7.1E-05	5.2E-05	1.2E-03	1.8E-03	6.4E-05
20	1.5E-04	1.1E-04	2.5E-03	3.8E-03	1.4E-04
25	1.9E-04	1.5E-04	3.3E-03	5.1E-03	1.8E-04
30	1.1E-04	8.3E-05	1.9E-03	2.8E-03	1.0E-04
Sum	5.4E-04	4.0E-04	9.1E-03	1.4E-02	4.9E-04
Life (years)	**1839**	**2494**	**110**	**72**	**2035**

Although the results show that the critical members have fatigue life greater than the expected service life, it cannot be concluded with 100% certainty that the structure would not sustain fatigue damage. The present analysis is carried out with the assumption that the weld connection between the chord and diagonal is flawless, which may not always be true. A survey conducted at University of Pittsburgh (Rizzo and Zhu 2010), asking the state DOTs to identify common problems that have occurred in highway sign support structures in their jurisdiction, resulted in several agencies reporting cracks in welds and loose or missing bolts. Also, the material investigation (electron microscopy) of the current truss conducted in the Centre for Materials and Sensor Characterization (Nims 2019) found poor quality welds with voids evident throughout the weld material. A debilitate connection like this is prone to fatigue failure and should be closely examined for fatigue cracks when performing the inspection of the support structures. To assess the effects of this weakening of the joints due to the poor quality of connections on the overall fatigue performance of the structure, fatigue life evaluation of the truss under simulated damaged states was carried out and is described in the next section.

4.2 Fatigue life in damaged state

This section deals with the fatigue life assessment of the truss in simulated damaged states. During the field inspection of the truss, two joints at the end of the truss were found to have failed. These joints were selected to introduce simulated damage in the truss. Three different damage scenarios – two with individual top and bottom joints damaged respectively, and third with both joints damaged – were considered. Damage at joints was simulated by reducing Young’s Modulus (E) of the members forming the joint. If a member is damaged at one end but sound on another, its E was reduced by 50% however, if a member is damaged at both ends, its E was reduced to zero. A reduction is E signifies that these members now have a lower load carrying capacity than they previously did. This would lead to a redistribution of stresses in the other members which is expected to affect the fatigue life of critical members. The three damage states along with affected members are depicted in Figure 4-8 through Figure 4-10.

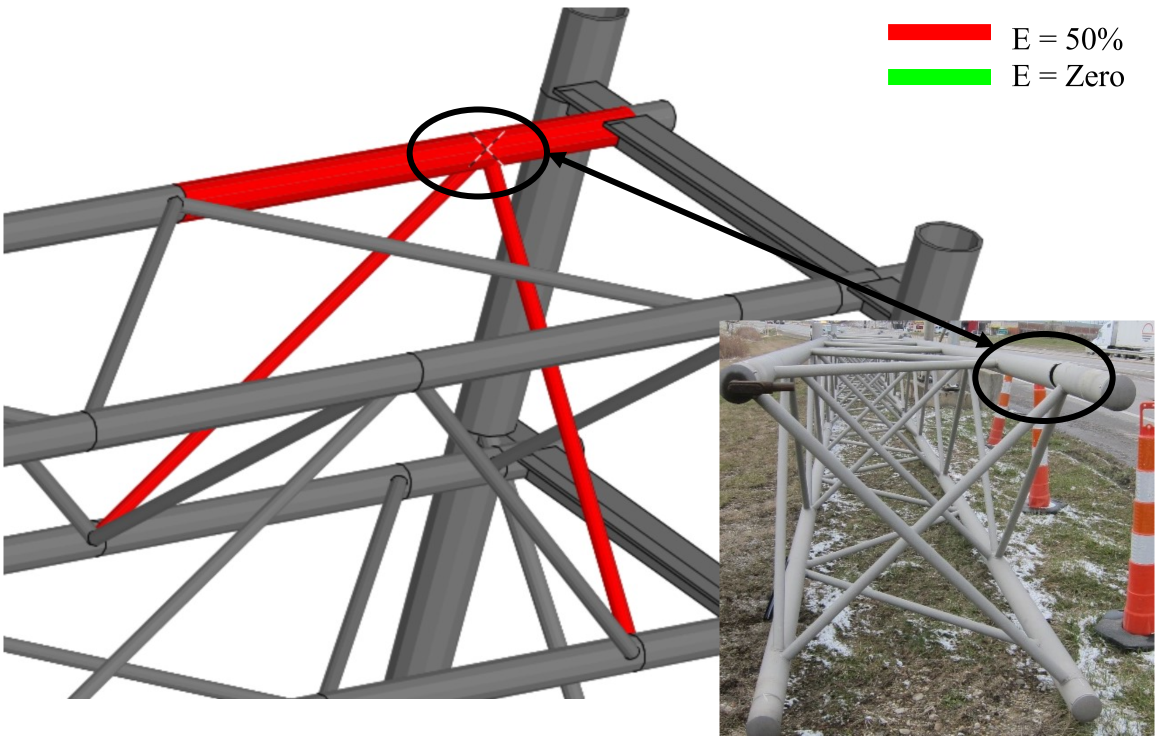

Figure 4-8: Damage scenario 1- Top joint damaged

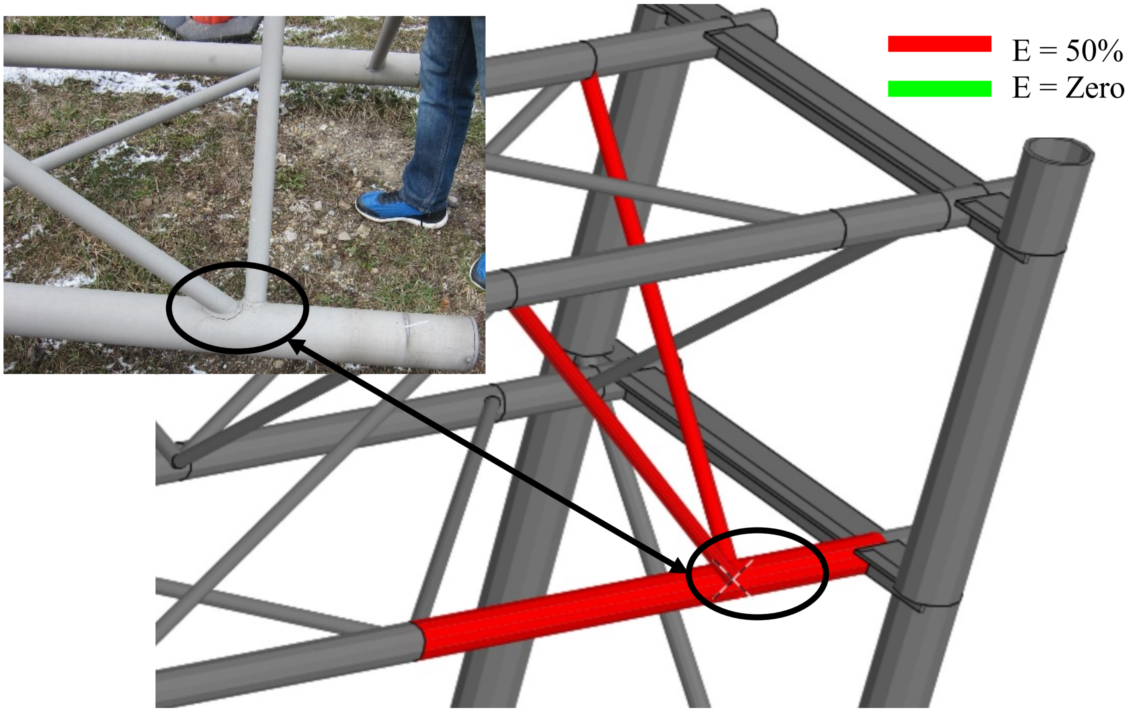

Figure 4-9: Damage scenario 2- Bottom joint damaged

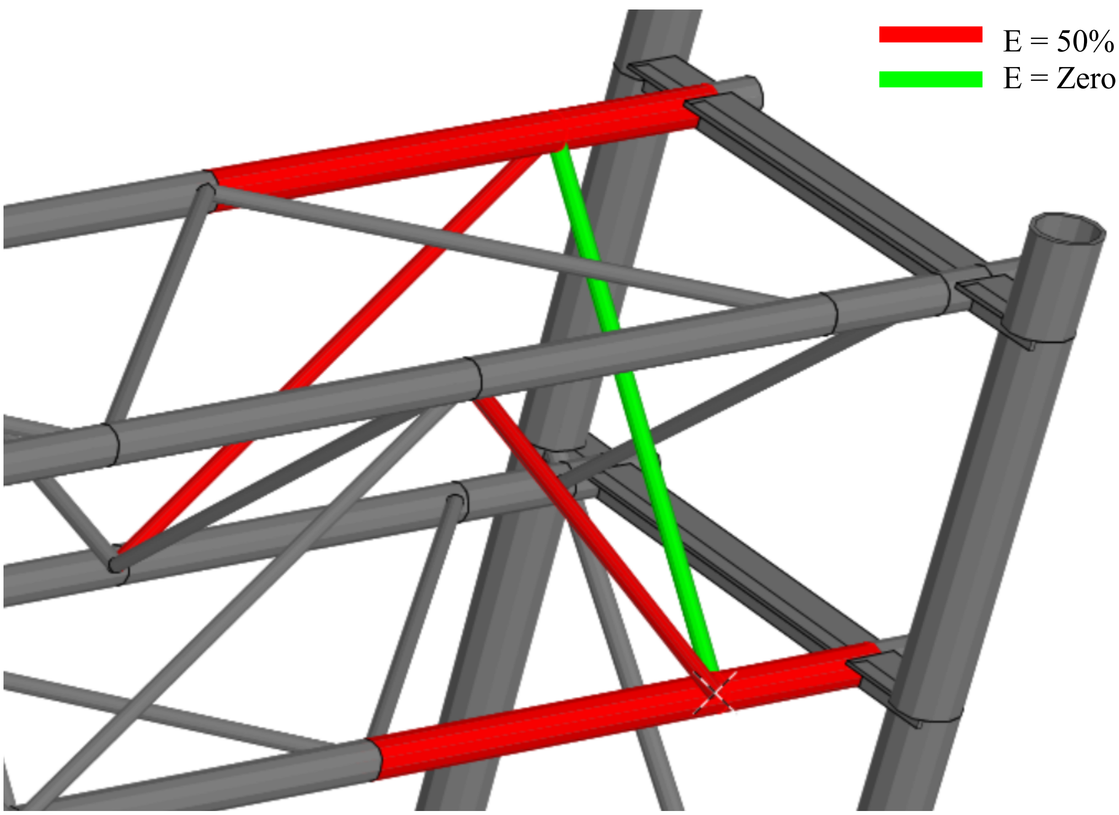

Figure 4-10: Damage scenario 3- Both joints damaged

4.2.1 Results

Similar procedure as described in section 4.1 was used to assess the fatigue performance in all the three damage scenarios. Fatigue life of the members shown in Figure 3-7 was evaluated again. This allowed comparison of damaged and undamaged scenarios. Results of fatigue life of critical members in damage scenarios one, two and three are shown in Table 4-7, Table 4-8, and Table 4-9 respectively .

The effective fatigue life of the structure in the three cases is found to be 65 years, 67 years and 64 years respectively which is only about 10% lower, then the fatigue life of undamaged structure (72 years). This shows that the truss is quite redundant and can sustain some damage without affecting the overall fatigue life of the structure.

Table 4-7: Fatigue life of critical members in damage scenarion-1 (Top joint damaged)

Wind speed	Total damage				
	Member 24	**Member 47**	**Member 71**	**Member 95**	**Member 97**
5	8.0E-08	4.3E-09	2.1E-06	1.9E-06	8.5E-09
10	1.6E-05	8.1E-07	4.1E-04	3.8E-04	1.6E-06
15	7.5E-05	4.0E-06	2.0E-03	1.9E-03	8.1E-06
20	1.6E-04	8.5E-06	4.1E-03	3.9E-03	1.7E-05
25	2.1E-04	1.2E-05	5.6E-03	5.2E-03	2.2E-05
30	1.2E-04	6.5E-06	3.2E-03	2.9E-03	1.3E-05
Sum	5.7E-04	3.2E-05	1.5E-02	1.4E-02	6.2E-05
Life (years)	**1741**	**31696**	**65**	**70**	**16214**

Table 4-8: Fatigue life of critical members in damage scenarion-2 (Bottom joint damaged)

Wind speed	Total damage				
	Member 24	**Member 47**	**Member 71**	**Member 95**	**Member 97**
5	7.1E-09	5.8E-08	2.1E-06	2.0E-06	8.9E-09
10	1.4E-06	1.1E-05	4.1E-04	3.9E-04	1.7E-06
15	6.8E-06	5.4E-05	2.0E-03	1.9E-03	8.3E-06
20	1.5E-05	1.2E-04	4.0E-03	4.0E-03	1.8E-05
25	1.9E-05	1.5E-04	5.4E-03	5.3E-03	2.4E-05
30	1.1E-05	8.6E-05	3.1E-03	2.9E-03	1.3E-05
Sum	5.3E-05	4.1E-04	1.5E-02	1.5E-02	6.5E-05
Life (years)	**19003**	**2414**	**67**	**69**	**15390**

Table 4-9: Fatigue life of critical members in damage scenarion-3 (Both joints damaged)

Wind speed	Total damage				
	Member 24	**Member 47**	**Member 71**	**Member 95**	**Member 97**
5	7.5E-09	4.5E-09	2.2E-06	2.0E-06	-
10	1.5E-06	8.3E-07	4.2E-04	3.9E-04	-
15	7.3E-06	4.2E-06	2.1E-03	1.9E-03	-
20	1.6E-05	9.0E-06	4.3E-03	4.1E-03	-
25	2.0E-05	1.2E-05	5.7E-03	5.4E-03	-
30	1.1E-05	6.7E-06	3.3E-03	3.0E-03	-
Sum	5.6E-05	3.3E-05	1.6E-02	1.5E-02	-
Life (years)	**17854**	**30757**	**64**	**68**	**-**

A comparison of the fatigue lives of critical members in undamaged and damages scenarios is presented in Table 4-10. Member 47 & 97 in scenario-1, member 24 & 97 in scenario-2, and members 24 & 47 in scenario-3 experience a more than tenfold increase in fatigue live in comparison to the undamaged structure. This is because these members constitute the damaged joint and their load carrying capacity was reduced to force the redistribution of stresses in the truss. All the other members that were not involved in the simulated damage, shows a decrease in fatigue life that varies from 2% (member 95 in damage scenario-1) to 42% (member 71 in damage scenario-3). However, the overall fatigue life of the truss sees a reduction of 8.5%, 6.4%, and 11% in damage scenarios one, two, and three respectively.

Table 4-10: Fatigue life comparison of undamaged and damages states

Damage Scenario	Fatigue life (years)				
	Member 24	**Member 47**	**Member 71**	**Member 95**	**Member 97**
Undamaged	1839	2494	110	72	2035
Scenario-1	1741	31696	65	70	16214
Scenario- 2	19003	2414	67	69	15390
Scenario- 3	17854	30757	64	68	NA

Chapter 5

Conclusion

5.1 Summary

The importance of non-cantilevered support structures in highway transportation is undeniable. With thousands of non-cantilevered trusses currently erected at various highways, several of which are in later half of their service life, it is very important to understand the behavior of these structures under different loading scenarios. This study investigates the response of an in-service non-cantilever highway truss on Alum Creek Drive at the interchange of Interstate 270, under the effects of natural wind gusts. A transient wind load time history was generated using Kaimal wind spectrum. The sample truss – a four chord box type – was modeled in SAP2000 and the wind loading time history was applied to it. Critical members susceptible to fatigue failure were identified and their stress time histories were extracted. Rainflow counting algorithm was employed to convert the variable amplitude stress cycles into several constant amplitude stress events and corresponding fatigue damage was evaluated using stress-life curves. Lastly, Palmgren Miner's rule of linear accumulation of damage was used to calculate the fatigue life of critical members. Both undamaged and damaged scenarios were considered. Damaged at joints was introduced in the model by reducing Young's modulus of the members and therefore reducing their load carrying capacity.

The results of this analysis found the fatigue life of all the critical members to be practically infinite. Undamaged state of the truss resulted in overall fatigue life of 141 years. Damages scenarios were found to have very little effect on the overall fatigue life of the structure. Compared to the undamaged state, the fatigue life in all three damage scenarios was reduced by less than 10%. Even though the findings of this report predict an infinite life of the structure, it should be noted that this result is only valid with the presumption that welded connections between members of the truss are sound and no defect in weld quality is considered in the present analysis.

The methodology, to evaluate the fatigue life of the overhead support structures, outlined in this study can easily be employed to any other type of structures as well. Geometry and material properties of the new structure need to be accurately modeled in any finite element software, wind speed distribution and wind load time history for the required location can be developed as described in section 4.1.1 and section 4.1.2 respectively. Once the analysis is performed and stress time histories of critical members are extracted, rainflow counting can be used to count stress cycles and finally appropriate stress-life curve, for the connection detail in question, along with Palmgren Miner's rule can be used to evaluate the fatigue life of the structure.

5.2 Conclusions

The results from the analytical wind analysis suggest that:

1. Maximum stresses in the truss occur at the two ends and are within the allowable limit for welded aluminum specified by AASHTO support specifications.
2. Fatigue life of the truss, under the effect of natural wind gustsexceeds the expected service life with the presumption that weld is sound. Structure is quite redundant and a partial damage at one or two joints causes little effect on the overall fatigue life of the truss.
3. Present fatigue analysis is performed assuming sound connections and no other factor except natural wind effecting fatigue performance. Several other factors such as diurnal temperature changes, truck gusts, subsequent corrosion of the members, weld deterioration etc., might affect the overall fatigue life of the structure.
4. Both the visual inspection of the truss as well as the study performed by Nims (Nims 2019) point to the fact that there were some problems with the weld fabrication that might have caused the premature failure of the structure.
5. The findings of this study are specific to the analyzed truss. It is uncertain if the same conditions prevail for other trusses is service. To gain an extended insight into the possibility of failure of such trusses, a larger sample size needs to be studied.
6. As such, the structures should be closely inspected for any defects on regular basis. Any damage found during inspection should be corrected to improve the performance of the structure.

5.3 Future work

The present study had several limitations due to time, resources, and scope of work. Recommendations for future studies addressing the issue of overhead support structures are made in this section.

1. Field instrumentation of the few representative structures can be done to gather stress-strain response of the structure. A better estimation of stress time history of the structure would allow the estimation of fatigue life with much more confidence.
2. Instead of the 'stick' model used in this study, a shell model of the truss can be developed. This would allow a more sophisticated modeling of the connection details and application of hotspot stress approach to assessing the fatigue life of the structure. Hotspot stress method considers stress concentration due to local geometry and is more accurate than the nominal stress method.
3. The analysis can be extended to other configurations such as a tube to gusset plate connection or angle to angle connection. This would allow an inclusive comparison of non-cantilevered support structures.
4. A parametric study addressing the effect of size on the fatigue life of tubular connections can be performed as the specified S-N curves for tubular connections are established based on experiments of a large specimen and do not account for size effect when applied to slender tubes.
5. S-N curve for AASHTO fatigue category ET can be established through experimental determination. This would result in improved fatigue life estimation for this class of fatigue details.

Bibliography

AASHO. (1961). “Specifications for the design and construction of structural supports for highway signs.” American Association of State Highway Officials, Washington, D.C.

AASHTO. (2012). *AASHTO LRFD Bridge Design Specifications*. American Association of State Highway and Transportation Officials, Washington, DC.

AASHTO. (2015). *LRFD Specifications for Structural Supports for Highway Signs, Luminaires, and Traffic Signals*. American Association of State Highway and Transportation Officials, Washington, DC.

American Welding Society. (2015). “Structural Welding Code-Steel.” American Welding Society, Miami, Florida.

Bannantine, J. A., Comer, J. J., and Handrock, J. L. (1990). *Fundamentals of metal fatigue analysis.* Prentice Hall, Englewood Cliffs, NJ.

Davenport, A. G. (1961). “The spectrum of horizontal gustiness near the ground in high winds.” *Quarterly Journal of the Royal Meteorological Society*, John Wiley & Sons, Ltd, 87(372), 194–211.

Dexter, R.J. and Fisher, J. W. (1999). “Fatigue and Fracture.” *Structural Engineering Handbook*, CRC Press, Boca Raton, Florida, 2592.

Dowling, N. E. (1993). *Mechanical behavior of materials*. Prentice Hall.

Eskandari, H., and Kim, H. S. (2017). “A Theory for Mathematical Framework and Fatigue Damage Function for the S-N Plane.” *Fatigue and Fracture Test Planning, Test Data Acquisitions and Analysis*, ASTM International, 100 Barr Harbor Drive, PO Box C700, West Conshohocken, PA 19428-2959, 299–336.

Fouad, Fouad H; Davidson, James; Delatte, Norbert; Calvert, E. (2003). *Structural*

Supports for Highway Signs, Luminaires, and Traffic Signals. *Transportation Research Board*, Washington, D.C.

Foutch, D., Rice, J., LaFave, J., Valdovinos, S., and Kim, T. (2006). *Evaluation of Aluminum Highway Sign Truss Designs and Standards for Wind and Truck Gust Loadings*. Urbana.

Ginal, S. (2003). "Fatigue Performance of Full-Span Sign Support Structures Considering Truck-Induced Gust And Natural Wind Pressures." *MS thesis*, Marquette University,Wisconsin, US.

Goodman, J. (1899). *Mechanics Applied to Engineering*. Longmans, Green and Co., London.

Hobbacher, A. (2015). *Recommendations for Fatigue Design of Welded Joints and Components*. IIW Collection, Springer International Publishing, Cham.

Holmes, J. (2001). *Wind Loading of Structures*. Taylor & Francis, New York, NY.

Huckelbridge, A. A., and Metzger, A. T. (2009). "Investigation of the Dayton, Ohio, IR 75 Sign Truss Failure of September 11, 2006." *Journal of Performance of Constructed Facilities*, 23(5), 372–378.

Iannuzzi, A., Spinelli, P., Iannuzzi, A., and Spinelli, P. (1987). "Artificial Wind Generation and Structural Response." *Journal of Structural Engineering*, 113(12), 2382.

Kaczinski. (1998). *Fatigue-resistant design of cantilevered signal, sign and light supports*. *Nchrp*.

Kaczinski, M. R., Dexter, R. J., and Van Dien, J. P. (1998). "Fatigue-resistant design of cantilevered signal, sign and light supports." *NCHRP Report*, National Academy Press, 176.

Kaimal, J. C., Wyngaard, J. C., Izumi, Y., and Coté, O. R. (1972). "Spectral characteristics of surface-layer turbulence." *Quarterly Journal of the Royal Meteorological Society*, John Wiley & Sons, Ltd, 98(417), 563–589.

KC, L. (2019). "Fatigue Calculation of Overhead Sign Structure for Thermal Loadings." University of Toledo.

Li, X., Whalen, T. M., and Bowman, M. D. (2006). “Fatigue Strength and Evaluation of Sign Structures, Volume 1: Analysis and Evaluation.” *Joint Transportation Research Program*, 1(June), 261.

Maddox, S. J. (2003). “Review of fatigue assessment procedures for welded aluminium structures.” *International Journal of Fatigue*, 25(12), 1359–1378.

MASHIRI, F. R., ZHAO, X.-L., HIRT, M. A., and NUSSBAUMER, A. (2007). “Size Effect of Welded Thin-Walled Tubular Joints.” *International Journal of Structural Stability and Dynamics*, 07(01), 101–127.

Nieslony, A. (2009). “Determination of fragments of multiaxial service loading strongly influencing the fatigue of machine components.” *MECHANICAL SYSTEMS AND SIGNAL PROCESSING*, 23(8), 2712–2721.

Nims, D. K. (2019). *Task 1 Final Report - Overhead Sign Failure Investigation*. Columbus, OH.

Rizzo, P., and Zhu, X. (2010). *Sensing Technology for Damage Assessment of Sign Supports and Cantilever Poles University of Pittsburgh*. *Draft Interim Report Contract No. 519691-PIT 008*, Pittsburgh, Pa.

Schumacher, A., Borges, L. C., and Nussbaumer, A. (2009). “A critical examination of the size effect correction for welded steel tubular joints.” *International Journal of Fatigue*, Elsevier Ltd, 31(8–9), 1422–1433.

Zielińska, M., and Zarychta, K. (2015). “A comparison of the wind spectrum according to different methods-an original project of a building on a cliff in Gdynia.” *International Journal of Applied Mechanics and Engineering*, 20(3), 663–672.

Appendix A

A1. Structural drawing of the truss

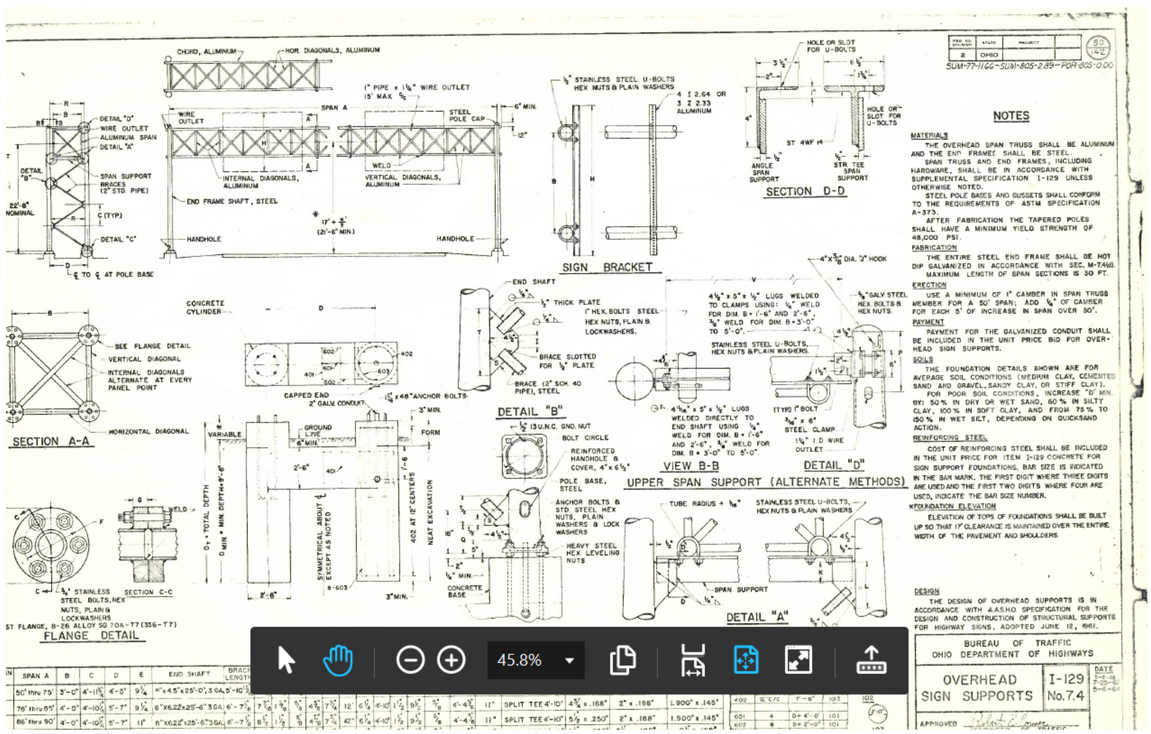

A2. Mat-lab script for wind time history

```
%This Mat-lab script is used to generate random wind load for 60 second
%period at various mean speeds. The generated load found at increments
%of 0.1 would be saved as text files to be imported in SAP2000


%establish input data and variables

U=input('Mean reference wind speed in mph:   ');%mean reference wind speed

Z_truss   = input('Height of truss above ground in ft:   '); %truss height

Cd      = 1.20;          %Coefficient of drag
```

```
A_big   = 7.525;         %Average area of bigger Signs
A_small= 1.394;          %Average area of smaller Signs
d_chord= 0.122;          %diameter of chord
T       = 60.0;          %Representative period(sec)
dt      = 0.1;           %Time increments(sec)
fL      = 0.1;           %Lower spectrum frequency bound(Hz)
fH      = 10;            %Upper spectrum frequency bound(Hz)
df      = 0.01;          %Frequency increment (Hz)
al      = 7;             %Power law exponent
K       = 0.4;           %The von Karman Constant (Liu, 1991)
z0      = 0.035;         %Terrain roughness for open terrain(m)(Liu, 1991)
%end of input
%Calculate mean component Uz at the height of truss
Z       = 10.0;          % Reference height (m)
Z_truss = Z_truss*12*0.0254;  %Convert height of truss to m
U     = (5280/3600*12*0.0254)*U; %mean reference speed (m/s)
Uz      = U*((Z_truss/Z1)^(1/al));      %Mean speed at truss height

%Creat spectral array of Kaimal spectrum using "for" loop
Ustar =  K*Uz/(log(Z/z0));               %Shear velocity U*
Num1 = 200.0*Z_truss*Ustar^2;            %Numerator of equation 2.4
i = 1;
  for f=fL:df:fH;                        %f is the frequency array
Num2(i) = Uz*(1.0+(50.0*f*Z)/(Uz))^(5/3);  %denominator of equation 2.4
      Sf(i)    = Num1/Num2(i);         %Kaimal spectrum array
      i= i+1;
  end
%Use WAWS method to calculate fluctuating component v'(t)
```

```
time=0:dt:T;                %time series of 601 time steps (60 seconds)

freq=fL:df:fH;              %frequency array

phi=2*pi*rand(1,991);        %an array of random numbers from 0 to 2*pi

for t=1:1:601;

    sum(t)=0;

    for j=1:1:991;           %Length of frequency array

    v(t)=((Sf(j)*freq(j)*df)^0.5)*cos(2.0*pi*freq(j)*time(t)+phi(j));

   %calculate the turbulent wind speed

   sum(t) = (2^0.5)*v(t) + sum(t);   %running sum of v' at all times

    end


    V(t)=sum(t)+Uz;    %sum both mean and fluctuating components of wind

    Pressure(t)=0.5*1.20*Cd*(V(t)^2);      %Calculate pressure

    Pressure_chord (t)=d_chord*Pressure(t)/1000;     %chord UDL in kN/m

end

     t1=rot90(time,3);

     p=rot90(Pressure,3);

     pc=rot90(Pressure_chord,3);


    save('C:\Users\AbdullahHaroon\OneDrive\School\Research\Sign
project\Fatigue\life evaluation\wind time history\time_step.txt','t1','-
ASCII')

    save('C:\Users\AbdullahHaroon\OneDrive\School\Research\Sign
project\Fatigue\life  evaluation\wind  time  history\pressure.txt','p','-
ASCII')

    save('C:\Users\AbdullahHaroon\OneDrive\School\Research\Sign
project\Fatigue\life  evaluation\wind time  history  \pressure_chord.txt'
,'pc','-ASCII')
```

A3. Mat-lab script for rainflow counting and damage calculation

```
%This script imports a data file containing time histories of individual
%members for all mean speeds and uses rainflow counting to calculate
%damage fractions. Rainflow counting algorithm used in this %script is
%adopted from the code written by Adam Nieslony (Nieslony 2009)and
%available to download from MathWorks website
%(https://www.mathworks.com/matlabcentral/fileexchange/3026-rainflow-
%counting-algorithm)

    x = importdata('TH_text\97.txt');   %import stress time history

    for i= 1:1:6             %create 6 arrays for all mean speeds
        b=x(1+(i-1)*601:601*i);

        y = sig2ext(b);             %Adopted from Nieslony 2009
        rf = rainflow(y);           %Adopted from Nieslony 2009

        s = size(rf,2);
        c = ones(1,s)*290;

        eff_stress = rf(2,:)*(c/(c-rf(3,:))); %Goodmen's relation for
                                               %effect of mean stress

        eff_stress_ksi = eff_stress*0.1450377;

        deno=eff_stress_ksi.^3.2895;
        num=ones(1,s)*(1.17*10^7);
        N = num./den;                     %Failure cycles (Ni)

        D = rf(3,:)./N;                   %damage fraction (ni/Ni)
        d(i,:)= sum(D);             %total damage at any mean speed
        d(i,:)

    end;
    xlswrite('damage97.xlsx',d)          %Save damage to excel file
    Total_damage = sum(d)
```